2. Tanaka H, Miake J, Notsu T, Sonyama K, Sasaki N, Iitsuka K, Kato M, Taniguchi S, Igawa O, Yoshida A, Shigemasa C, Hoshikawa Y, Kurata Y, Kuniyasu A, Nakayama H, Inagaki N, Nanba E, Shiota G, Morisaki T, Ninomiya H, Kitakaze M, Hisatome I. Proteasomal degradation of Kir6.2 channel protein and its inhibition by a Na+ channel blocker aprindine. *Biochem Biophys Res Commun.* 2005;331:1001-1006.
3. Hirota Y, Kurata Y, Kato M, Notsu T, Koshida S, Inoue T, Kawata Y, Miake J, Bahrudin U, Li P, Hoshikawa Y, Yamamoto Y, Igawa O, Shirayoshi Y, Nakai A, Ninomiya H, Higaki K, Hiraoka M, Hisatome I. Functional stabilization of Kv1.5 protein by Hsp70 in mammalian cell lines. *Biochem Biophys Res Commun.* 2008;372:469-474.
4. Koshida S, Kurata Y, Notsu T, Hirota Y, Kuang TY, Li P, Bahrudin U, Harada S, Miake J, Yamamoto Y, Hoshikawa Y, Igawa O, Higaki K, Soma M, Yoshida A, Ninomiya H, Shiota G, Shirayoshi Y, Hisatome I. Stabilizing effects of eicosapentaenoic acid on Kv1.5 channel protein expressed in mammalian cells. *Eur J Pharmacol.* 2009;604:93-102.
5. Claycomb WC, Lanson NA Jr, Stallworth BS, Egeland DB, Delcarpio JB, Bahinski A, Izzo NJ Jr. HL-1 cells: a cardiac muscle cell line that contracts and retains phenotypic characteristics of the adult cardiomyocyte. *Proc Natl Acad Sci USA.* 1998;95:2979-2984.
6. Woods AJ, Robert MS, Choudhary J, Barry ST, Mazaki Y, Sabe H, Morley SJ, Critchley DR, Norman JC. Paxillin associates with poly (A)-binding protein 1 at the dense endoplasmic reticulum and the leading edge of migrating cells. *J Biol Chem.* 2002;277:6428-6437.
7. Toyota F, Ding WG, Zankov DP, Omatsu-Kanbe M, Isono T, Horie M, Matsuura H. Chearaterization of the rapidly activating delayed rectifier potassium current, I_{Kr}, in Hl-1 mouse atrial myocytes. *J membrane Biol.* 2010;235:73-87.
8. Xia M, Salata JJ, Figueroa DJ, Lawlor AM, Liang HA, Liu Y, Connolly TM. Functional expression of L- and T-type Ca2+ channels in murine HL-1 cells. *J Mol Cell Cardiol.* 2004;36:111-119.
9. Sartiani L, Bochet P, Cerbai E, Mugelli A, Fischmeister R. Functional expression of the hyperpolarization-activated, non-selective cation current I(f) in immortalized HL-1 cardiomyocytes. *J Physiol.* 2002;545:81-92.

Downloaded from circres.ahajournals.org at SHIGA UNIVERSITY OF MEDICAL SCIENCE on January 6, 2011

Circulation Journal
Official Journal of the Japanese Circulation Society
http://www.j-circ.or.jp

ORIGINAL ARTICLE
Arrhythmia/Electrophysiology

Atrioventricular Block-Induced Torsades de Pointes With Clinical and Molecular Backgrounds Similar to Congenital Long QT Syndrome

Yuko Oka, MD; Hideki Itoh, MD, PhD; Wei-Guang Ding, MD, PhD; Wataru Shimizu, MD, PhD; Takeru Makiyama, MD, PhD; Seiko Ohno, MD, PhD; Yukiko Nishio, MD; Tomoko Sakaguchi, MD, PhD; Akashi Miyamoto, MD; Mihoko Kawamura, MD; Hiroshi Matsuura, MD, PhD; Minoru Horie, MD, PhD

Background: Atrioventricular block (AVB) sometimes complicates QT prolongation and torsades de pointes (TdP).

Methods and Results: The clinical and genetic background of 14 AVB patients (57±21 years, 13 females) who developed QT prolongation and TdP was analyzed. Electrophysiological characteristics of mutations were analyzed using heterologous expression in Chinese hamster ovary cells, together with computer simulation models. Every patient received a pacemaker or implantable cardioverter defibrillator; 3 patients had recurrence of TdP during follow-up because of pacing failure. Among the ECG parameters, QTc interval was prolonged to 561±76 ms in the presence of AVB, but shortened to 495±42 ms in the absence of AVB. Genetic screening for *KCNQ1*, *KCNH2*, *SCN5A*, *KCNE1*, and *KCNE2* revealed four heterozygous missense mutations of *KCNQ1* or *KCNH2* in 4 patients (28.6%). Functional analyses showed that all mutations had loss of functions and various gating dysfunctions of I_{Ks} or I_{Kr}. Finally, action potential simulation based on the Luo-Rudy model demonstrated that most mutant channels induced bradycardia-related early afterdepolarizations.

Conclusions: Incidental AVB, as a trigger of TdP, can manifest as clinical phenotypes of long QT syndrome (LQTS), and that some patients with AVB-induced TdP share a genetic background with those with congenital LQTS. (*Circ J* 2010; **74:** 2562–2571)

Key Words: Atrioventricular block; Ion channels; Long QT syndrome; Torsades de pointes

The acquired form of long QT syndrome (LQTS) is a major cause of torsades de pointes (TdP),[1,2] which results from various factors, including drugs, bradycardia or hypokalemia. Regarding bradycardia, Kurita et al demonstrated that patients with bradycardia-induced TdP display abnormally prolonged QT intervals at slower heart rates (<60 beats/min) than those without TdP.[3] Some groups have reported the genetic background of bradycardia-induced TdP, as well as of congenital LQTS. In 2001, we reported a female with 2:1 atrioventricular block (AVB) and TdP, in whom the *KCNH2* A490T mutant was identified as heterozygous.[4] Subsequently, Lupoglazoff et al demonstrated that, in neonates, LQTS with 2:1 AVB is associated with *KCNH2* mutations whereas sinus bradycardia-related LQTS is associated with *KCNQ1* mutations.[5] Chevalier et al reported that among 29 patients with complete AVB and a QT interval >600 ms, 5 (17%) had mutations on genes encoding K^+ channels, and the expression test of these mutations showed functional changes compared with the wild-type (WT) K^+ current.[6]

Editorial p 2546

In Japan, some papers on congenital LQTS have been published,[2,7–9] but the molecular pathogenesis of AVB-related TdP has not been fully examined, particularly with respect to the relationship between genotype and cellular electrophysiology. The aim of this study was to investigate gene mutations and clarify their functional outcome in con-

Received May 31, 2010; revised manuscript received July 30, 2010; accepted August 2, 2010; released online October 21, 2010 Time for primary review: 16 days

Department of Respiratory and Cardiovascular Medicine (Y.O., H.I., T.S., A.M., M.K., M.H.), Department of Physiology (W.-G.D., H.M.), Shiga University of Medical Science, Otsu; Division of Cardiology, Division of Arrhythmia and Electrophysiology, Department of Cardiovascular Medicine, National Cerebral and Cardiovascular Center, Suita (W.S.); and Department of Cardiovascular Medicine, Kyoto University Graduate School of Medicine, Kyoto (T.M., S.O., Y.N.), Japan

Mailing address: Minoru Horie, MD, PhD, Department of Respiratory and Cardiovascular Medicine, Shiga University of Medical Science, Seta Tsukinowa-cho, Otsu 520-2192, Japan. E-mail: horie@belle.shiga-med.ac.jp

ISSN-1346-9843 doi:10.1253/circj.CJ-10-0498

All rights are reserved to the Japanese Circulation Society. For permissions, please e-mail: cj@j-circ.or.jp

secutive AVB patients complicated with TdP.

Methods

Study Population

The study cohort contained 14 consecutive probands, from unrelated families, who showed a prolonged QT interval and TdP associated with AVB. They were referred to 3 institutes in Japan; Shiga University of Medical Science (Otsu), National Cardiovascular Center (Suita), and Kyoto University Graduate School of Medicine (Kyoto) for LQTS genetic testing between 1996 and 2008.

Clinical Characterization

In each case, we recorded 12-lead electrocardiograms (ECGs) before and after AVB episodes, as well as gathering the results from other cardiovascular examinations and detailed clinical evaluations. Prolonged QT interval was diagnosed by the presence of prolongation of ventricular repolarization (corrected QT interval [QTc] >460ms in lead V_5, according to Bazett's formula).[10] We excluded cases of TdP caused by AVB with drugs associated with QT prolongation, as well as those with active ischemia detected by noninvasive or invasive tests, including coronary angiography. We also investigated cardiac events in all 14 probands and their family members. Cardiac events were syncope, TdP, ventricular fibrillation (VF), aborted cardiac arrest (requiring defibrillation) or sudden cardiac death. We also followed the therapies and clinical prognoses of these patients.

Genetic Analysis

Genomic DNA was isolated from venous blood by QIAamp DNA blood midikit (Qiagen, Hilden, Germany). Established primer settings were used to amplify the entire coding regions of the known LQTS genes (*KCNQ1*, *KCNH2*, *SCN5A*, *KCNE1*, and *KCNE2*). Denaturing high-performance liquid chromatography (WAVE system Model 3500, Transgenomic, Omaha, NE, USA) was performed as described elsewhere, and abnormal conformers were amplified by polymerase chain reaction (PCR), and sequenced with an ABI PRISM-3130 sequencer (Perkin-Elmer Applied Biosystems, Wellesley, MA, USA). If we detected mutations in these genes, family members associated with the probands were also genetically analyzed. Formal informed consent was obtained from each patient or their guardians according to standards approved by local institutional review boards.

Expression Plasmids

The expression plasmids, pIRES2-EGFP/*KCNQ1*(wild-type; WT/*KCNQ1*) and pRc-CMV/*KCNH2* (WT/*KCNH2*) were kindly provided by Dr Barhanin (Université de Nice, Sophia Antipolis, Valbonne, France) and Dr Sanguinetti (University of Utah, Salt Lake City, UT, USA), respectively. The mutations were introduced using overlap PCR. The mutant plasmids were constructed by substituting the 838-bp *Xho*I-*Bgl*II for the G272V mutant, 464-bp *Hin*dIII-*Bst*XI for the D111V mutant, 1458-bp *Bst*XI-*Bgl*II for the A490T mutant, or 592-bp *Fse*I-*Sbf*I fragments for the P846T mutant for the corresponding fragments of WT/*KCNQ1* or WT/*KCNH2*. The nucleotide sequence of the construct was confirmed prior to the expression studies.

Expression in Chinese Hamster Ovary (CHO) Cells

CHO cells were maintained in Dulbecco's modified Eagle's medium and Ham's F12 nutritional mixture (Gibco-BRL, Rockville, MD, USA) supplemented with 10% fetal bovine serum (Gibco-BRL) and antibiotics (100U/ml penicillin and 100μg/ml streptomycin) in a humidified incubator gassed with 5% CO_2 and 95% air at 37°C. CHO cells were transiently transfected using 1μg of WT/*KCNQ1* or mutant/*KCNQ1*, and 1μg of pIRES-CD8/*KCNE1* per 35-mm dish, using the LipofectAMINE method according to the manufacturer's instructions (Invitrogen, Carlsbad, CA, USA). In some experiments, 0.5μg of WT/*KCNQ1* was transfected with or without mutant/*KCNQ1*, instead of 1μg of WT/*KCNQ1*. Cells successfully transfected with both *KCNQ1* and *KCNE1* cDNA were selected by green fluorescent protein (GFP) and decoration with anti-CD8 antibody-coated beads (Dynabeads CD8; Dynal Biotech, Oslo, Norway). The cells were transiently transfected with either WT/*KCNH2* or mutant/*KCNH2*, using the LipofectAMINE method according to the manufacturer's instructions. For a 35-mm dish the amount of plasmid was 2μg and 0.175μg of GFP; only GFP-positive cells were used for the patch-clamp study.

Electrophysiological Experiments

Whole-cell patch-clamp recordings were conducted at 37.0±1.0°C using an EPC-8 patch-clamp amplifier (HEKA, Lambrecht, Germany) 48–72h after transfection. No leak subtraction was used. The normal Tyrode solution contained (in mmol/L): NaCl 140, KCl 5.4, $CaCl_2$ 1.8, $MgCl_2$ 0.5, NaH_2PO_4 0.33, glucose 5.5, and HEPES 5 (pH adjusted to 7.4 with NaOH). The pipette solution contained (in mmol/L): potassium aspartate 70, KCl 40, KH_2PO_4 10, EGTA 5, $MgSO_4$ 1, Na_2-ATP (Sigma, St Louis, MO, USA) 3, Li_2-GTP 0.1, and HEPES 5 (pH adjusted to 7.4 with KOH). A coverslip with adherent CHO cells was placed on the bottom of a glass recording chamber (0.5ml in volume) mounted on the stage of an inverted microscope (TE2000-U, Nikon, Tokyo, Japan). Pipette resistance was 3–5MΩ when filled with internal solution. Currents and voltages were digitized and voltage commands were generated through an LIH-1600 AD/DA interface (HEKA) controlled by PatchMaster software (HEKA). Current amplitude was divided by membrane capacitance (Cm) to obtain current densities (pA/pF) in each cell. The voltage-dependence of current activation was determined by fitting the normalized tail current (I_{tail}) vs test potential (V_{test}) to a Boltzmann function:

$$I_{tail} = 1/(1+\exp[(V_{0.5}-V_t)/k]),$$

where $V_{0.5}$ indicates the voltage at which the current is half-maximally activated and k is the slope factor.

Computer Simulation of Action Potential Duration (APD)

Ventricular action potentials were simulated by using the dynamic Luo-Rudy model with recent modifications.[11,12] The ratio of I_{Kr} and I_{Ks} conductance was set at 23:1, 17:1, and 19:1 in the epicardium, endocardium, and M cell layer, respectively. Based on the experimental data of voltage-clamp recordings of *KCNH2* channels heterologously expressed in CHO cells, we constructed Markov or Hodgkin-Huxley models for simulated mutant channels as compared with mutants associated with congenital LQTS. In order to construct mutant channel models, we decreased the conductance of each channel as appropriate for the decreased current density, and looked for adequate changes in mutant channels by changing each coefficient value, in turn, for gating states associated with impaired gating defects. The simulation for voltage-clamp experiments was calculated using the 4th-order Runge-Kutta method with a fixed-time step of

Table 1. Clinical Characteristics and Gene Mutations of Probands With Bradycardia-Induced Torsades de Pointes

Case no.	Age (years)	Sex (M/F)	Diagnosis	Cardiac events	Family history	ECG at AVB		ECG without AVB		Therapy	Follow-up		Mutation/Gene
						QTc (ms)	HR (beats/min)	QTc (ms)	HR (beats/min)		Period (months)	Arrhythmic events	
1	27	F	2:1 AVB	TdP	–	600	50	545	71	PM	41	None	A490T/KCNH2
2	74	F	CAVB	TdP	–	NA	NA	NA	NA	PM	22	None	
3	73	M	CAVB	TdP	–	635	39	NA	NA	PM	104	None	
4	57	F	CAVB	TdP	–	525	43	545	61	ICD, BB, Ib	96	None	D111V/KCNH2
5	69	F	2:1 AVB	TdP	–	452	45	476	86	PM, BB, Ib	84	None	
6	21	F	Wenckebach AVB	TdP	Sudden death	625	65	489	75	ICD, Ib	79	VF because of Wenckebach AVB	
7	76	F	2:1 AVB	TdP	–	578	50	424	83	PM, BB	59	None	G272V/KCNQ1
8	71	F	CAVB	TdP	–	729	57	489	72	ICD	46	None	P846T/KCNH2
9	73	F	CAVB	TdP	–	567	33	NA	NA	PM	129	None	
10	62	F	CAVB	TdP	–	473	29	NA	NA	PM	277	None	
11	68	F	CAVB	TdP	–	552	39	NA	NA	PM	207	TdP because of V pacing failure	
12	38	F	CAVB	TdP	Mother with LQTS	493	28	500	65	PM, BB	NA	NA	
13	76	F	CAVB	TdP	–	500	46	NA	NA	PM	57	TdP because of low back-up rate	
14	18	F	CAVB	TdP	–	570	47	NA	NA	PM	130	None	
Ave±SD	57±21					561±76	44±11	495±42	64±27		102±71		

AVB, atrioventricular block; TdP, torsades de pointes; PM, pacemaker; CAVB, complete atrioventricular block; NA, not available; ICD, implantable cardioverter defibrillator; BB, β-blocker; Ib, class Ib antiarrhythmic drugs; VF, ventricular fibrillation.

0.02 ms. The simulation programs were coded in C++ and implemented for personal computers.[12]

Statistical Analysis

Numerical data are presented as mean±standard error of the mean. Student's t-test was used to compare the data between different groups for electrophysiological measurement, and differences were considered significant at $P<0.05$.

Results

Clinical Characteristics of the Patients in This Study

The clinical characteristics of the 14 patients enrolled in the study are presented in **Table 1**. The mean age at the onset of AVB was 57±21 years, and 13 patients (92.8%) were females. All patients showed TdP with AVB: 10 had complete AVB, 3 had 2:1 AVB, and 1 had Wenckebach AVB. No patient had experienced syncope or ventricular arrhythmias prior to the appearance of TdP. One patient (case 6 in **Table 1**) with Wenckebach AVB had 2 family members who had suddenly died at the age of 1 year and 3 months, respectively. The mother of case 12 (**Table 1**) had atrial fibrillation, mitral regurgitation, and complete AVB with prolonged QT interval, but no TdP.

In most patients with AVB-related TdP, the tachyarrhythmia started from premature ventricular contractions after a long-pause interval following ventricular arrhythmias, so-called "TdP from short–long–short pattern" (**Figure 1D**).[13] The ECGs available at the time of AVB showed severely prolonged QT interval (heart rate 44±11 beats/min and QTc 561±76 ms). On the other hand, the ECGs without AVB available in 7 cases also showed a prolonged QT interval (heart rate 64±27 beats/min, $P<0.05$, and QTc 495±42 ms, P=NS, vs those in AVB). ECGs in sinus rhythm were obtained in 4 and 3 patients before and after AVB, respectively.

All patients underwent implantation of either an implantable cardioverter-defibrillator (ICD) or permanent pacemaker (PM), together with the administration of several drugs, including β-blockers (ICD n=3; PM n=11). Mean clinical follow-up during advanced therapy was 102±71 months. After the placement of a PM or ICD, 2 patients maintained own ventricular beats but the other 12 depended on ventricular pacing during the follow-up period. Three patients had recurrence of TdP even while receiving treatment. Patient no. 11 suddenly experienced repetitive TdP because of pacing failure and no. 13 also experienced TdP when her own ventricular beats had been set faster than the basal pacing rate. In patient 6, the reappearance of Wenckebach AVB without ventricular pacing caused ventricular tachycardia. In all 3 cases, no gene mutations were detected.

Molecular Genetics and Clinical Characteristics of Patients With Gene Mutations

The genetic analysis revealed different heterozygous mutations in 4 (28.6%) of 14 AVB-related TdP cases (**Table 1**): 1 *KCNQ1* mutation, G272V, and 3 *KCNH2* mutations, D111V, A490T and P846T (**Figure 1A**). All were located in the nonpore regions; G272V is located in the S5 domain for the *KCNQ1* channel; D111V, A490T, and P846T are located in the N-terminus, S2–S3 inner loop, and C-terminal domains for the *KCNH2* channel, respectively (**Figure 1B**). In the remaining 10 patients, we were unable to detect any mutations associated with the 5 major LQTS-related genes.

G272V in *KCNQ1* (Case 7 in Table 1) The G272V muta-

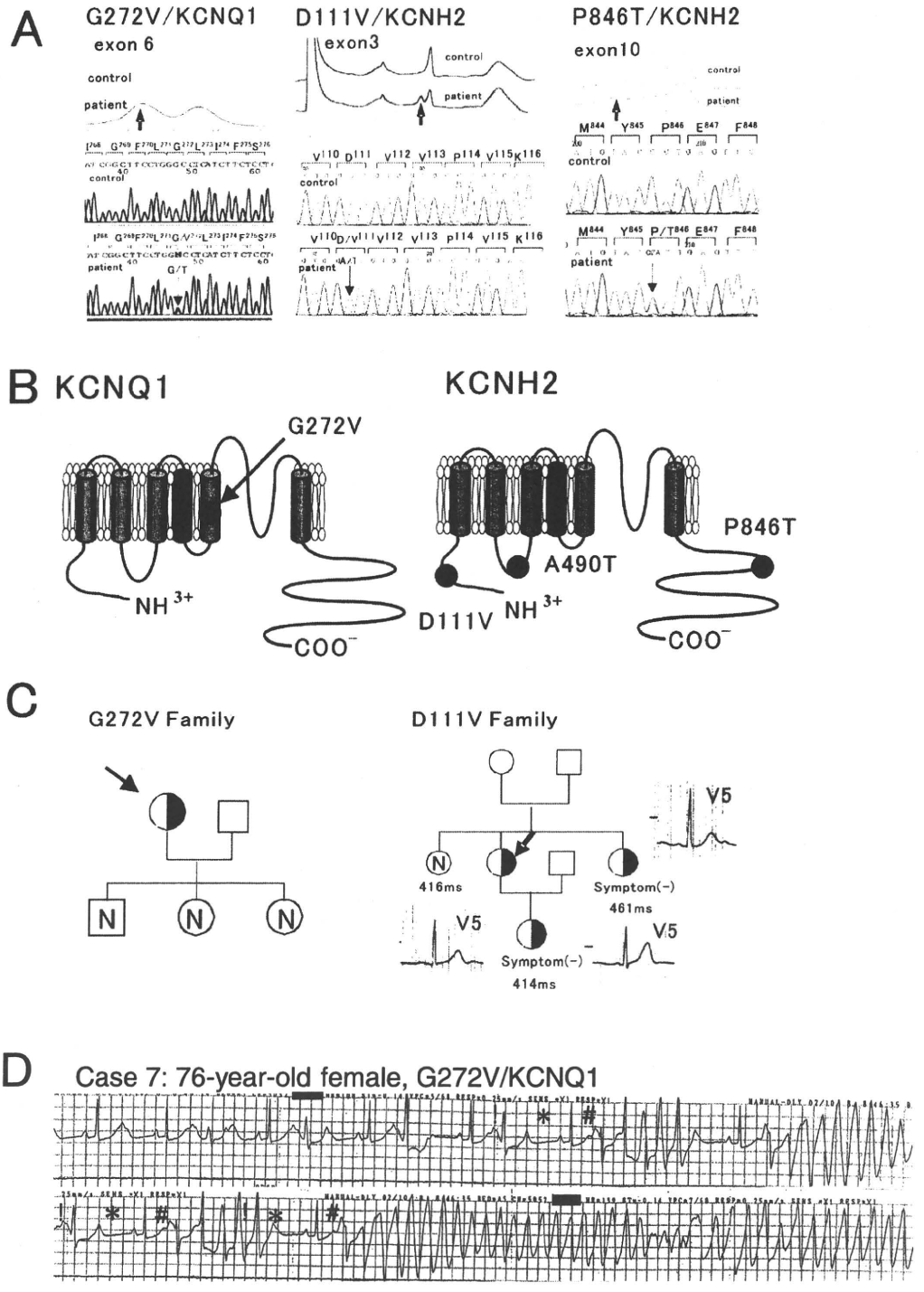

Figure 1. Molecular discovery and clinical data associated with *KCNQ1* and *KCNH2* mutations, and the initiation of atrioventricular block -related torsades de pointes (TdP). (**A**) Denaturing high-performance liquid chromatography patterns and DNA sequence data in normal controls and patients with G272V for *KCNQ1* (**Left**), D111V for *KCNH2* (**Middle**), and P846T for *KCNH2* (**Right**). (**B**) Schemes showing the topology of cardiac ion channel proteins for *KCNQ1* and *KCNH2* and the location of mutations identified in this study. (**C**) Two pedigrees of G272V and D111V families. Circles and squares represent female and male family members, respectively; probands are indicated by arrows. Heterozygous carriers are represented as half-filled symbols, family members in whom no genetic data were available are shown by open symbols, and non-carriers by open symbols with N. QTc intervals corrected by Bazzet's formula in lead V5 are given for each available family member. (**D**) Representative ECG recordings from case 7 (76-year-old female with G272V-KCNQ1 mutation). TdP during 2:1 AV block started with so-called "short (!)–long (*)–short (#) pattern" which resulted in a long pause (*).[13]

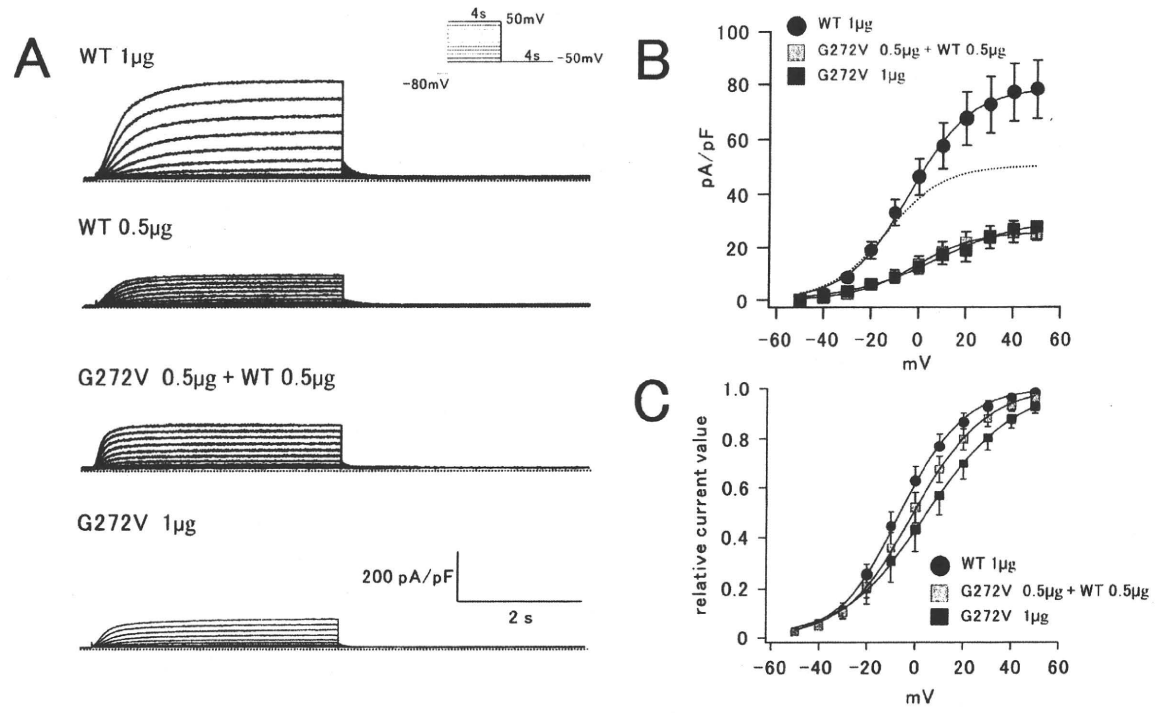

Figure 2. G272V KCNQ1 mutant channel shows loss of function associated with decreased density on I_{Ks}. Functional analyses on wild-type (WT) and G272V mutant channels expressed in Chinese Hamster ovary cells. (**A**) Representative current recordings for each channel. Currents were elicited from a holding potential of –80 mV, by depolarizing pulses (4-s duration) from –50 to +50 mV (with a 10-mV step increment) and subsequent repolarization to –50 mV for a 4-s duration (inset). Concentrations of cDNAs used for transfection are indicated near each graph. (**B**) Tail current-voltage relationships for 1 μg WT (closed circles; n=18), 0.5 μg WT (indicated by dotted line; n=14), 0.5 μg WT plus 0.5 μg G272V (green squares; n=19), 1 μg G272V (red squares; n=11). (**C**) Normalized activation curves by fitting to Boltzmann function.

tion was identified in a 76-year-old female who did not have a particularly relevant family history (**Figure 1A Left panel**). For approximately 10 years, she had taken nilvadipine and gliclazide because of hypertension and diabetes mellitus. Approximately 1 year before hospitalization, her QTc interval was within normal range (424 ms). When she was admitted to hospital because of syncope, her monitoring ECGs displayed 2:1 AVB (50 beats/min), prolonged QTc interval (578 ms), and repetitive TdP (**Figure 1D**). Her serum K^+ level was low (2.5 mEq/L). Because AVB persisted, she underwent DDD PM implantation. After correction of the serum K^+ level and PM therapy, her QTc interval shortened and TdP disappeared. She was free from cardiac events for the following 59 months. The genetic analysis revealed 3 children as non-mutation carriers (**Figure 1C Left panel**).

D111V in *KCNH2* (Case 4 in Table 1) The D111V mutation was identified in a 57-year-old female who did not have a particularly relevant family history (**Figure 1A Middle panel**). She experienced syncope after eating breakfast, and the monitoring ECG in the ambulance documented complete AVB (43 beats/min), prolonged QTc interval (525 ms) and TdP. After external PM therapy was initiated, TdP disappeared. She then underwent ICD implantation and started oral mexiletine hydrochloride (300 mg/day) and propranolol hydrochloride (30 mg/day); she has had no cardiac events over a follow-up period of 96 months. However, her QTc interval has remained prolonged even in the absence of AVB (545 ms, 4 years later). The genetic tests in her 3 relatives showed 2 mutation carriers (**Figure 1C Right panel**): a 51-year-old sister and 29-year-old daughter. Both these relatives were asymptomatic. Her daughter's QTc interval was within normal range (414 ms), but the sister's was prolonged (461 ms).

P846T in *KCNH2* (Case 8 in Table 1) The P846T mutation was found in a 71-year-old female who did not have a particularly relevant family history (**Figure 1A Right panel**). She experienced syncope after breakfast, and the monitoring ECG in the ambulance displayed complete AVB (45 beats/min) and repetitive TdP with prolonged QT interval. On admission, her AV conduction resumed at 57 beats/min, but her QTc interval remained prolonged (729 ms). After ICD implantation, she was free from cardiac events for 46 months, but her QTc interval remained prolonged (489 ms). We did not conduct a genetic analysis in this family.

A490T in *KCNH2* (Case 1 in Table 1) We have previously reported the clinical features of a A490T mutation identified in a 27-year-old female.[3] Briefly, her 12-lead ECG showed severe bradycardia because of 2:1 AVB (50 beats/min) with complete left bundle branch block and remarkable prolongation of QTc interval (600 ms). She fainted and collapsed while talking on the telephone, and the Holter ECG showed TdP associated with 2:1 AVB.

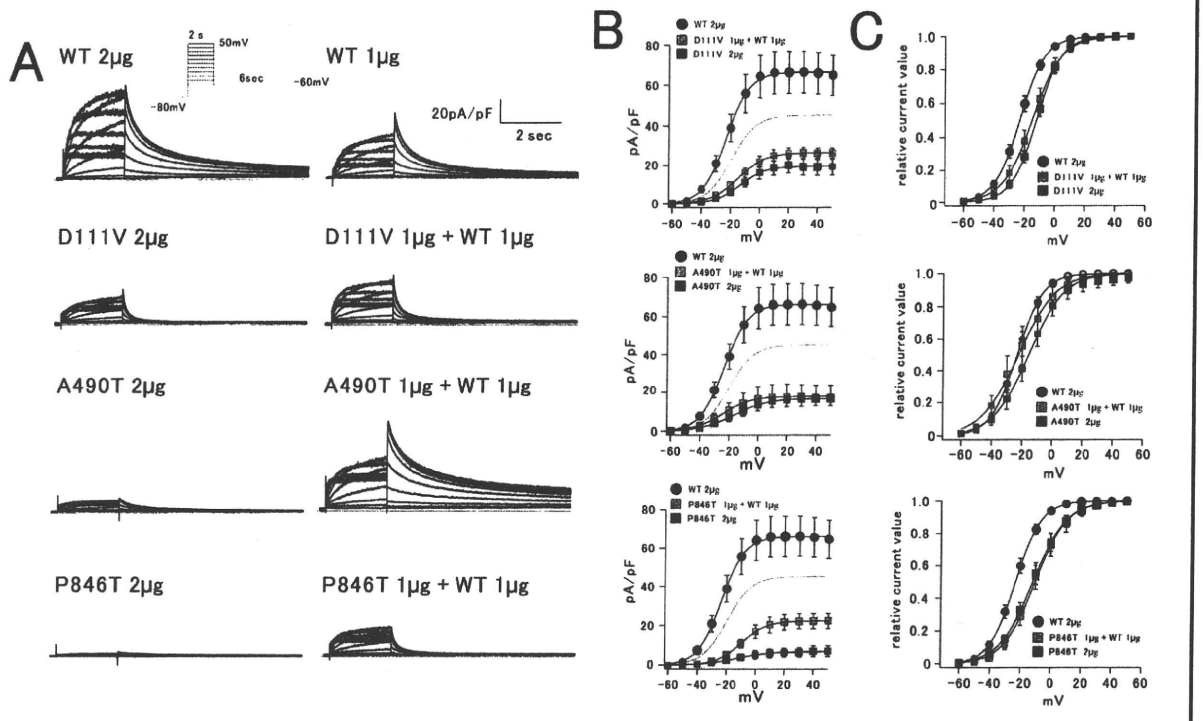

Figure 3. All *KCNH2* mutant channels show loss of function associated with decreased density on I_{Kr}. Electrophysiological characteristics of *KCNH2* mutant channels in Chinese Hamster ovary cells. (**A**) Families of representative current traces. Experimental protocol is shown in the inset. Concentrations of cDNAs used for transfection are indicated above each graph. (**B**) Tail current-voltage relationships for 2 μg wild-type (WT: closed circles; n=20), 1 μg WT (dotted line; n=14), 1 μg WT plus 1 μg mutant (green squares; n=10–13), 2 μg mutant (red squares; n=8–12). (**C**) Normalized activation curves by fitting to Boltzmann function.

Table 2. Parameters of Inactivation in WT and Mutant *KCNH2*

	WT (n=16)	WT/D111V (n=16)	D111V (n=15)	WT/A490T (n=17)	A490T (n=15)	WT/P846T (n=15)	P846T (n=16)
$V_{0.5}$ (mV)	−58.3±4.7	−40.1±4.1**	−47.4±7.0	−32.5±3.9*	−44.2±3.3	−38.7±2.4**	−55.5±3.5
Slope factor	29.2±1.4	33.9±1.3	35.3±1.7**	30.6±1.4†	34.9±1.1**	33.0±0.6†	37.5±1.7*

*P<0.001 vs WT, **P<0.01 vs WT, †P<0.05 vs WT.
WT, wild-type.

Expression Study

In order to clarify the functional consequences of the G272V mutation of *KCNQ1* and the D111V, A490T, and P846T mutations of *KCNH2*, we assessed the electrophysiological properties of the WT and mutant clones by using CHO cells.

Biophysical Assay of *KCNQ1* Mutant Channel Figure 2A shows representative examples of whole-cell currents recorded from CHO cells transfected with WT/*KCNQ1*, G272V/*KCNQ1* alone or WT co-expressed G272V/*KCNQ1* (WT/G272V) plus *KCNE1*. CHO cells transfected with WT/*KCNQ1* (1 or 0.5 μg) displayed outward currents with slow activation/deactivation kinetics on depolarization, which are typical of I_{Ks} currents, as previously reported.[14,15] In contrast, a cell transfected with G272V/*KCNQ1* (1 μg) displayed smaller I_{Ks} currents compared with that of the WT (1 μg). WT/G272V at an equimolar ratio (0.5 μg) also showed smaller I_{Ks} currents.

In Figure 2B, the tail current densities at −50 mV measured in multiple cells are plotted as a function of test pulse voltages (between −50 and +50 mV). The tail current densities at −50 mV after depolarizing test pulses to +40 mV were 77.0±11 pA/pF for 1 μg WT (n=18), 49.5±7.9 pA/pF for 0.5 μg WT (n=14), 25.4±4.5 pA/pF for 0.5 μg WT/G272V (n=19) (vs WT 1 μg, P<0.001), 26.7±4.9 pA/pF for 1 μg G272V (n=11) (vs WT 1 μg, P<0.01). Thus, compared with the WT I_{Ks} current, co-transfection of the mutant affected the expressed current densities.

Figure 2C represents the voltage-dependence of current activation. Tail current densities after each test potential were fitted to a Boltzmann function (see Methods). The parameters were $V_{0.5}$=−5.2±3.0 mV, k=11.1±0.6 for 1 μg WT, $V_{0.5}$=−1.0±3.7 mV, k=11.7±1.1 for 0.5 μg WT/G272V, $V_{0.5}$=5.7±5.4 mV, k=14.3±1.6 (vs WT 1 μg; P<0.05) for 1 μg G272V. Regarding half-activation voltages, WT plus G272V and G272V tended to shift to the depolarization side compared with WT but there was no statistical significance. In

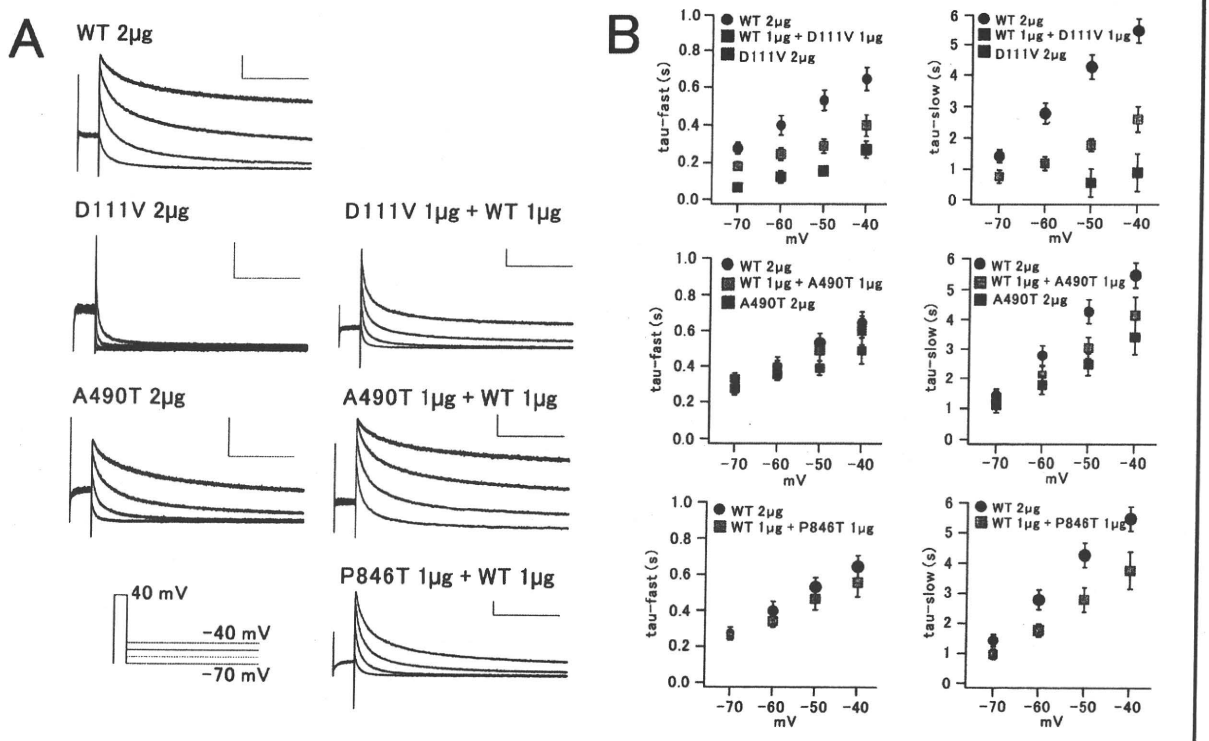

Figure 4. *KCNH2* mutant channels show a faster deactivation. (**A**) Representative tail currents elicited after depolarization to +40 mV (inset protocol). (**B**) Deactivation process was fitted to 2 components having different time constants, tau-fast and tau-slow. They were calculated in a pooled data from multiple cells transfected by 3 mutants (from top of panel B, D111V, A490T and P846T, respectively) and are plotted against membrane potentials (–70 to –40), for 2 μg WT (closed circles; n=15), 1 μg WT plus 1 μg mutant (green squares; n=7–14 for each channel), 2 μg mutant (red squares; n=6–8).

slope factors, G272V alone channel was larger than WT ($P<0.05$). Overall, the most important finding was the dominant-negative effect for the G272V channel.

Biophysical Assay of 3 *KCNH2* Mutant Channels Figure 3A shows representative examples of whole-cell currents recorded from CHO cells transfected with WT/*KCNH2* (2 and 1 μg), mutant/*KCNH2* (2 μg), or WT co-expressed mutant/*KCNH2* (WT/mutant) (1 μg each). CHO cells transfected with WT/*KCNH2* (2 or 1 μg, **Figure 3A Upper 2 panels**) displayed outward currents with inward rectifying properties, which are typical of I_{Kr} currents.[16] In contrast, the magnitude of currents from cells expressing all of the WT/mutants and mutant only were remarkably reduced (**Figure 3A Lower 6 panels**).

In **Figure 3B**, the tail current densities at –60 mV are plotted as a function of test pulse voltages (between –60 and +50 mV). The mean current densities after depolarizing test pulse to +20 mV in WT channels were 66.2±11 pA/pF for 2 μg (n=20) and 45.0±9.3 pA/pF for 1 μg (n=14). In contrast, those in the WT/mutant and mutant channels were 25.1±2.9 pA/pF in WT/D111V (n=13), 15.8±6.0 pA/pF in WT/A490T (n=10), 20.5±3.9 pA/pF in WT/P846T (n=12), 18.8±3.6 pA/pF for D111V (n=9), 15.2±3.4 pA/pF for A490T (n=12), 6.1±2.3 pA/pF for P846T (n=8), respectively. They were all significantly smaller than those of the 2-μg WT channels (vs WT 2 μg; $P<0.01$). **Figure 3C** shows that all WT/mutant and mutant channels tended to shift to the depolarization side compared with the WT. Overall, all mutant channels showed loss of function associated with a dominant-negative effect and shift of the activation curve to depolarization.

We then examined whether the mutations affected the inactivation kinetics of mutant channels using a double-pulse protocol. $V_{0.5}$ and the slope factor of steady-state inactivation differed between WT and WT plus mutant or mutant. All mutant *KCNH2* channels showed the shift of inactivation curves to depolarizing direction, and the differences were statistically significant (**Table 2**). Therefore, we also changed the parameters associated with inactivation states in the following simulation study.

Figure 4A depicts original current traces showing deactivation at 4 different repolarization potentials (from –70 to –40 mV) of WT and/or mutant/*KCNH2*. Deactivating currents were best fit with a double-exponential function, and are summarized in **Figure 4B**. At 4 different potentials, both time constants (Tau-fast and Tau-slow) for D111V and WT/D111V were smaller than those of the WT. Tau-slow of WT/P846T was also smaller than those of the WT. We could not assess that of P846T (2 μg), because it was too small to measure. In contrast, there were no significant changes between the WT and WT/A490T or A490T in the deactivation process.

Computer Simulation of APD

In order to compare how functional changes caused by mutations affect ventricular action potentials, a simulation study

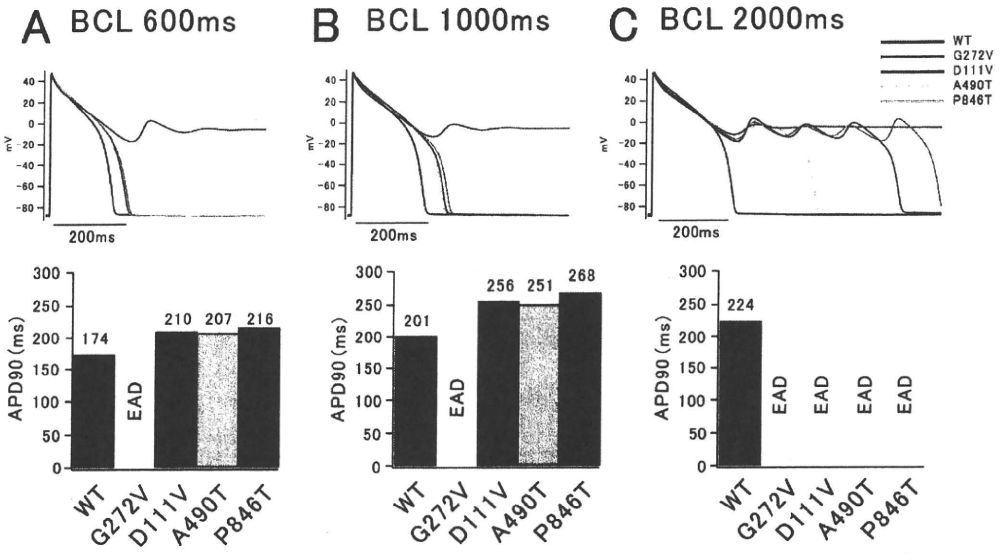

Figure 5. Computer simulations with Luo-Rudy myocardial model show bradycardia-induced early afterdepolarization (EAD). Each figure presents (**A**) action potential duration (APD) at basic cycle length (BCL) of 600 ms, (**B**) APD at BCL of 1,000 ms, and (**C**) APD at BCL of 2,000 ms. The longer the BCL in each model was, the more the APD was prolonged. EADs appeared in the models of D111V/WT, A490T/WT, and P846T/WT only at BCL of 2,000 ms, but appeared at all BCLs in the case of G272V/WT.

Table 3. Parameters of Simulation Data in Bradycardia-Induced Long QT Syndrome

Gene	Mutation	WT basal parameters	Mutant changed parameters
KCNQ1	G272V	gsk=0.202*(1+0.6/(1+pow(0.000038/cai),1.4)))	gsk=0.067*(1+0.6/(1+pow(0.000038/cai),1.4)))
		xs1 ss=1/(1+exp(-(v-1.5)/16.7))	xs1 ss=1/(1+exp(-(v-6.5)/16.7))
KCNH2	D111V	gherg=0.0135*pow(Kout,0.59)	gherg=0.331*0.0135pow(Kout,0.59)
		$\alpha\alpha$=65.5e-3*exp(0.05547153*(v-36))	$\alpha\alpha$=65.5e-3*exp(0.05547153*(v-69))
		αi=0.439*exp(–0.02352*(v+25))*4.5/Kout	αi=0.439*exp(–0.02352*(v+3))*4.5/Kout
		$\beta\beta$=2.9375e-3*exp(–0.02158*v)	$\beta\beta$=2*2.9375e-3*exp(–0.02158*v)
KCNH2	A490T	gherg=0.0135*pow(Kout,0.59)	gherg=0.1887*0.0135pow(Kout,0.59)
		αi=0.439*exp(–0.02352*(v+25))*4.5/Kout	αi=0.439*exp(–0.02352*(v-6))*4.5/Kout
KCNH2	P846T	gherg=0.0135*pow(Kout,0.59)	gherg=0.265*0.0135pow(Kout,0.59)
		$\alpha\alpha$=65.5e-3*exp(0.05547153*(v-36))	$\alpha\alpha$=65.5e-3*exp(0.05547153*(v-80))
		αi=0.439*exp(–0.02352*(v+25))*4.5/Kout	αi=0.439*exp(–0.02352*(v+3))*4.5/Kout
		$\beta\beta$=2.9375e-3*exp(–0.02158*v)	$\beta\beta$=1.3*2.9375e-3*exp(–0.02158*v)

was conducted using the Luo-Rudy model, which incorporated the Markov[13] or Hodgkin-Huxley[17] process gating for the mutant channels (**Figure 5**). **Table 3** shows the parameters of simulation that were changed to fit to experimental results. We simulated action potentials in all myocardial layers at 3 different basic cycle lengths (BCL 600, 1,000, 2,000 ms) (**Figures 5A–C**). In the endocardium and epicardium, APD of all mutant models was prolonged, but did not produce early afterdepolarizations (EAD) (data not shown in **Figure 5**). In contrast, in the simulated M cell layer, APD was lengthened significantly at a slower heart rate. In the lower half of **Figure 5**, below each simulated action potential, the corresponding bar graphs show APDs at 90% repolarization. Three APD models with D111V, A490T, and P846T displayed EADs at BCL of 2,000 ms, whereas G272V displayed it at all BCLs.

Discussion

There are 3 major findings in the present study. (1) In 4 of 14 consecutive AVB-associated TdP patients, 3 *KCNH2* and 1 *KCNQ1* heterozygous missense mutations were identified. (2) Electrophysiological analyses revealed loss of function associated with decreased current densities and various dysfunctions on I_{Ks} or I_{Kr} in 4 mutants. (3) Functional changes reconstituted by the computer simulation resulted in a prolonged APD and EAD under condition of bradycardia.

During AVB, our 14 patients showed a prolonged QT interval and TdP. Based on a comparison of ECGs available before and after AVB, we found the QT intervals were lengthened even in the absence of AVB. These clinical characteristics indicate that AVB-related TdP might share a similar genetic background with congenital LQTS: mutations on cardiac ion channel genes could be partially causative. Lupo-

glazoff et al[5] demonstrated that in neonates that, while LQTS with 2:1 AVB is associated with *KCNH2* mutations, sinus bradycardia-related LQTS is associated with *KCNQ1* mutations. In 9 of 10 cases, 2:1 AVB-induced LQTS could be caused by LQTS-related gene mutations. In contrast, Chevalier et al found 4 K^+ channel gene mutations in 5 of 29 adult patients with AVB-induced LQTS (17.3%).[6] Our cohort also consisted of adult LQTS patients, with a mutation rate of 28.6%. This prevalence rate was similar to Chevalier's report, but lower than that in the 2:1 AVB-related LQTS in neonates. These studies have shown that AVB-induced LQTS in neonates has a stronger genetic association than AVB-induced LQTS in adults. Regarding the diagnostic rate of genetic testing in general, no candidate mutations could be detected in 30–40% of congenital LQTS cases. In contrast, it has been shown recently that genetic polymorphisms modify the QT interval.[18–24] Although we did not check polymorphisms in the present study, it is possible that our subjects might have some modifier-gene mutations. Thus, it remains possible that the remaining 10 patients in our study without apparent genetic variants may have as yet unknown variants.

In our cohort, it was difficult to prove the efficacy of β-blockers because very few patients were taking these drugs. In order to investigate the efficacy of β-blockers it will be necessary to study more cases with AVB-induced TdP. The first step in the treatment of all patients with AVB-induced TdP is the implantation of a device. Although PM implantation as first-line therapy for AVB-induced TdP is not disputed, 3 of our patients had a recurrence of TdP after the device was implanted, because of inadequate ventricular pacing, suggesting that AVB patients with TdP require strict PM management. In cases of persistent QT prolongation, even after PM therapy, it might become necessary to consider ICD implantation.

Several AVB-related gene mutations have been functionally assayed:[6] 3 *KCNH2* mutations, R328C, R696C and R1047L, were shown to have no strong dominant-negative effects on I_{Kr}. Another *KCNE2* mutation (R77W), which was identified in an AVB patient while taking flecainide, exerted no effects on I_{Kr}. Overall, previous analyses of mutations have shown them to cause only mild functional change. Our study showed similar results; all 4 mutants displayed loss of function associated with decreased densities on I_{Ks} or I_{Kr}, which were basically similar to those in congenital LQTS. On average, our patients experienced TdP at 57 years of age, which is older than the mean age of onset reported for those with congenital LQTS. Mutation carriers, who remain asymptomatic well into adulthood, may incidentally have fatal events in the presence of additional triggers, such as AVB.[25]

Several mutations of *SCN5A*, coding the α-subunit of Na^+ channels, have been found in newborn and infant cases of long QT.[26–28] They showed functional 2:1 AVB caused by profound QT prolongation. Therefore, the pathological basis differs between those cases and ours. Irrespective of genetic testing results, our patients who developed TdP in the presence of AVB showed QT prolongation, even in sinus rhythm. Thus, AVB may not be directly associated with QT prolongation, but the bradycardia caused by AVB enhances it and eventually leads to TdP. Our computer simulation study showed that, at a slower heart rate, APD lengthened significantly, suggesting that AVB-related bradycardia could exacerbate QT prolongation.

Study Limitation

Female sex is a predisposing factor for the development of cardiac arrhythmic events in patients with congenital and acquired LQTS, as previous reports have demonstrated.[29–31] In our study, almost all patients (93%) were also female, and therefore it would be possible that not only AVB but female sex affected cardiac repolarization and ventricular irritability in our cohort.

Conclusion

This study showed that incidental AVB as a trigger of TdP could manifest as clinical phenotypes of LQTS, and that some patients with AVB-induced TdP could have genetic backgrounds associated with congenital LQTS-related genes.

Acknowledgments

We thank Ms Arisa Ikeda for excellent technical assistance. This work was supported by a Grant-in-Aid for Scientific Research from the Japan Society for the Promotion of Science and the Biosimulation and Health Sciences Research Grant from the Ministry of Health, Labor, and Welfare of Japan, and grants from the Uehara Memorial Foundation (M.H.) and the Grant-in-Aid for Young Scientists from the Ministry of Education, Culture and Technology of Japan (H.I.).

References

1. Moss A, Kass R. Long QT syndrome: From channels to cardiac arrhythmias. *J Clin Invest* 2005; **115:** 2018–2024.
2. Shimizu W. Clinical Impact of Genetic Studies in Lethal Inherited Cardiac Arrhythmias. *Circ J* 2008; **72:** 1926–1936.
3. Kurita T, Ohe T, Marui N, Aihara N, Takaki H, Kamakura S, et al. Bradycardia-induced abnormal QT prolongation in patients with complete atrioventricular block with torsades de pointes. *Am J Cardiol* 1992; **69:** 628–633.
4. Yoshida H, Horie M, Otani H, Kawashima T, Onishi Y, Sasayama S. Bradycardia-induced long QT syndrome caused by a de novo missense mutation in the S2-S3 inner loop of HERG. *Am J Med Genet* 2001; **98:** 348–352.
5. Lupoglazoff JM, Denjoy I, Villain E, Fressart V, Simon F, Bozio A, et al. Long QT syndrome in neonates: Conduction disorders associated with HERG mutations and sinus bradycardia with KCNQ1 mutations. *J Am Coll Cardiol* 2004; **43:** 826–830.
6. Chevalier P, Bellocq C, Millat G, Piqueras E, Potet F, Schott JJ, et al. Torsades de pointes complicating atrioventricular block: Evidence for a genetic predisposition. *Heart Rhythm* 2007; **4:** 170–174.
7. Nagaoka I, Shimizu W, Itoh H, Yamamoto S, Sakaguchi T, Oka Y, et al. Mutation site dependent variability of cardiac events in Japanese LQT2 form of congenital long-QT syndrome. *Circ J* 2008; **72:** 694–699.
8. Makita N. Phenotypic overlap of cardiac sodium channelopathies. *Circ J* 2009; **73:** 810–817.
9. Ogawa K, Nakamura Y, Terano K, Ando T, Hishitani T, Hoshino K. Isolated non-compaction of the ventricular myocardium associated with long QT syndrome. *Circ J* 2009; **73:** 2169–2172.
10. Bazett HC. An analysis of the time relations of electrocardiograms. *Heart* 1920; **7:** 353–370.
11. Clancy CE, Rudy Y. Na^+ channel mutation that causes both Brugada and long-QT syndrome phenotypes: A simulation study of mechanism. *Circulation* 2002; **105:** 1208–1213.
12. Itoh H, Sakaguchi T, Ding WG, Watanabe E, Watanabe I, Nishio Y, et al. Latent genetic background and molecular pathogenesis of drug-induced long QT syndrome. *Circ Arrhythmia Electrophysiol* 2009; **2:** 511–523.
13. Tan HL, Bardai A, Shimizu W, Moss AJ, Schulze-Bahr E, Noda T, et al. Genotype-specific onset of arrhythmias in congenital long-QT syndrome. *Circulation* 2006; **114:** 2096–2103.
14. Barhanin J, Lesage F, Guillemare E, Fink M, Lazdunski M, Romey G. KvLQT1 and lsK (minK) proteins associate to form the I_{Ks} cardiac potassium current. *Nature* 1996; **384:** 78–80.
15. Sanguinetti MC, Curran ME, Zou A, Shen J, Spector PS, Atkinson DL, et al. Coassembly of KvLQT1 and minK (I_{sK}) proteins to form cardiac I_{Ks} potassium channel. *Nature* 1996; **384:** 80–83.
16. Sanguinetti MC, Jiang C, Curran ME, Keating MT. A mechanistic link between an inherited and an acquired cardiac arrhythmia: *HERG* encodes the I_{Kr} potassium channels. *Cell* 1995; **81:** 299–307.

17. Hodgkin AL, Huxley AF. A quantitative description of membrane current and its application to conduction and excitation in nerve. *J Physiol* 1952; **117:** 500–544.
18. Newton-Cheh C, Guo CY, Larson MG, Musone SL, Surti A, Camargo AL, et al. Common genetic variant in KCNH2 is associated with QT interval duration: The Framingham Heart Study. *Circulation* 2007; **116:** 1128–1136.
19. Plant LD, Bowers PN, Liu Q, Morgan T, Zhang T, State MW, et al. A common cardiac sodium channel variant associated with sudden infant death in African Americans, SCN5A S1103Y. *J Clin Invest* 2006; **116:** 430–435.
20. Nishio Y, Makiyama T, Itoh H, Sakaguchi T, Ohno S, Gong YZ, et al. D85N, a KCNE1 polymorphism, is a disease-causing gene variant in long QT syndrome. *J Am Coll Cardiol* 2009; **54:** 812–819.
21. Newton-Cheh C, Eijgelsheim M, Rice KM, de Bakker PI, Yin X, Estrada K, et al. Common variants at ten loci influence QT interval duration in the QTGEN study. *Nat Genet* 2009; **41:** 399–406.
22. Pfeufer A, Sanna S, Arking DE, Müller M, Gateva V, Fuchsberger C, et al. Common variants at ten loci modulate the QT interval duration in the QTSCD study. *Nat Genet* 2009; **41:** 407–414.
23. Arking DE, Pfeufer A, Post W, Kao WH, Newton-Cheh C, Ikeda M, et al. A common genetic variant in the NOS1 regulator NOS1AP modulate cardiac repolarization. *Nat Genet* 2006; **38:** 644–651.
24. Crotti L, Monti MC, Insolia R, Peljto A, Goosen A, Brink PA, et al. NOS1AP is a genetic modifier of the long-QT syndrome. *Circulation* 2009; **120:** 1657–1663.
25. Sakaguchi T, Shimizu W, Itoh H, Noda T, Miyamoto Y, Nagaoka I, et al. Hydroxyzine, a first generation H(1)-receptor antagonist, inhibits human ether-a-go-go-related gene (HERG) current and causes syncope in a patient with the HERG mutation. *J Pharmacol Sci* 2008; **108:** 462–471.
26. Lupoglazoff JM, Cheav T, Baroudi G, Berthet M, Denjoy I, Cauchemez B, et al. Homozygous SCN5A mutation in long-QT syndrome with functional two-to-one atrioventricular block. *Circ Res* 2001; **89:** E16–E21.
27. Chang CC, Acharfi S, Wu MH, Chiang FT, Wang JK, Sung TC, et al. A novel SCN5A mutation manifests as a malignant form of long QT syndrome with perinatal onset of tachycardia/bradycardia. *Cardiovasc Res* 2004; **64:** 268–278.
28. Miura M, Yamagishi H, Morikawa Y, Matsuoka R. Congenital long QT syndrome and 2:1 atrioventricular block with a mutation of the SCN5A gene. *Pediatr Cardiol* 2003; **24:** 70–72.
29. Nakamura H, Kurokawa J, Bai CX, Asada K, Xu J, Oren RV, et al. Progesterone regulates cardiac repolarization through a nongenomic pathway: An in vitro patch-clamp and computational modeling study. *Circulation* 2007; **116:** 2913–2922.
30. Makkar RR, Fromm BS, Steinman RT, Meissner MD, Lehmann MH. Female gender as a risk factor for torsades de pointes associated with cardiovascular drugs. *JAMA* 1993; **270:** 2590–2597.
31. Locati EH, Zareba W, Moss AJ, Schwartz PJ, Vincent GM, Lehmann MH, et al. Age- and sex-related differences in clinical manifestations in patients with congenital long-QT syndrome: Findings from the International LQTS Registry. *Circulation* 1998; **97:** 2237–2244.

Progress in Neuro-Psychopharmacology & Biological Psychiatry 34 (2010) 401–405

Contents lists available at ScienceDirect

Progress in Neuro-Psychopharmacology & Biological Psychiatry

journal homepage: www.elsevier.com/locate/pnp

QTc prolongation and antipsychotic medications in a sample of 1017 patients with schizophrenia

Yuji Ozeki [a,b,*], Kumiko Fujii [a], Naoki Kurimoto [c], Naoto Yamada [c], Masako Okawa [d], Takesuke Aoki [e], Jun Takahashi [e], Nobuya Ishida [f], Minoru Horie [g], Hiroshi Kunugi [b]

[a] Department of Psychiatry, Dokkyo University School of Medicine, 880 Kitakobayashi, Mibu, 321-0293, Japan
[b] Department of Mental Disorder Research, National Institute of Neuroscience, National Center of Neurology and Psychiatry, 4-1-1, Ogawahigashimachi, Kodaira, Tokyo, 187-8502, Japan
[c] Department of Psychiatry, Shiga University of Medical Science, Setatsukinowacyo, Otsu, 520-2121, Japan
[d] Department of Sleep Medicine, Shiga University of Medical Science, Setatsukinowacyo, Otsu, 520-2121, Japan
[e] Minakuchi Hospital, 2-2-43, Minakuchihonnmachi, Kouka, 528-0031, Japan
[f] Biwako Hospital, 1-8-5, Sakamoto, Otsu, 520-0113, Japan
[g] Department of Cardiovascular and Respiratory Medicine, Shiga University of Medical Science, Setatsukinowacyo, Otsu, 520-2121, Japan

ARTICLE INFO

Article history:
Received 8 September 2009
Received in revised form 11 January 2010
Accepted 11 January 2010
Available online 15 January 2010

Keywords:
Antipsychotics
QT prolongation
Schizophrenia
Sudden death

ABSTRACT

Many antipsychotic drugs cause QT prolongation, although the effect differs based on the particular drug. We sought to determine the potential for antipsychotic drugs to prolong the QTc interval (>470 ms in men and >480 ms in women) using the Bazett formula in a "real-world" setting by analyzing the electrocardiograms of 1017 patients suffering from schizophrenia. Using logistic regression analysis to calculate the adjusted relative risk (RR), we found that chlorpromazine (RR for 100 mg = 1.37, 95% confidence interval (CI) = 1.14 to 1.64; $p<.005$), intravenous haloperidol (RR for 2 mg = 1.29, 95% CI = 1.18 to 1.43; $p<.001$), and sultopride (RR for 200 mg = 1.45, 95% CI = 1.28 to 1.63; $p<.001$) were associated with an increased risk of QTc prolongation. Levomepromazine also significantly lengthened the QTc interval. The second-generation antipsychotic drugs (i.e., olanzapine, quetiapine, risperidone, and zotepine), mood stabilizers, benzodiazepines, and antiparkinsonian drugs did not prolong the QTc interval. Our results suggest that second-generation antipsychotic drugs are generally less likely than first-generation antipsychotic drugs to produce QTc interval prolongation, which may be of use in clinical decision making concerning the choice of antipsychotic medication.

© 2010 Elsevier Inc. All rights reserved.

1. Introduction

QTc interval prolongation is associated with presyncope, syncope, polymorphic ventricular tachycardia, the subtype torsade de pointes, and sudden cardiac death (Faber et al., 1994). Previous studies have indicated an increased risk of sudden cardiac death in patients treated with antipsychotics (Hennessy et al., 2002; Ray et al., 2001; Straus et al., 2004). A retrospective cohort study of 481,744 Tennessee Medicaid enrollees, of whom 1487 died from sudden cardiac death, found that current moderate-dose antipsychotic use (>100 mg of thioridazine equivalents) increased the rate of sudden cardiac death (multivariate risk ratio of 2.39), when compared with the nonuse of antipsychotics (Ray et al., 2001). A cohort study of three U.S. medical programs found that patients with treated schizophrenia had higher rates of cardiac arrest and ventricular arrhythmia than did controls (patients with glaucoma and those with psoriasis), with risk ratios ranging from 1.7 to 3.2 (Hennessy et al., 2002). A study of 554 sudden cardiac death subjects reported that the current use of antipsychotics was associated with a three-fold increased risk of cardiac death (Straus et al., 2004).

Although torsade de pointes and sudden death are rare, rate-corrected QT (QTc) prolongation serves as a risk factor for these conditions. In a study of 495 psychiatric patients receiving various psychotropic drugs and 101 healthy reference individuals, 8% of patients showed QTc prolongation (>456 ms) (Reilly et al., 2000). Advanced age (>65 years), as well as the use of tricyclic antidepressants, thioridazine, and droperidol were indicated as robust predictors of QTc lengthening (Reilly et al., 2000). High antipsychotic doses were also associated with QTc prolongation (Reilly et al., 2000). In a sample of 111 psychiatric inpatients receiving a median daily dose of more than 600 mg [chlorpromazine (CP) equivalent] of antipsychotics, 90% had schizophrenia or related psychoses, and 23% showed QTc interval of >420 ms, whereas only 2% of unmedicated controls did (Warner et al., 1996). However, there is little clinical data to aid in assessing the

Abbreviations: QTc, rate-corrected QT; 95% CI, 95% confidence interval; HPD, haloperidol; HPDiv, intravenous injection of haloperidol; RR, relative risk; ECG, electrocardiogram; SGAs, second-generation antipsychotics; FGAs, first-generation antipsychotics; DSM-IV, Diagnostic and Statistical Manual of Mental Disorders, 4th ed.; CP, chlorpromazine; LP, levomepromazine; OR, odds ratio.

* Corresponding author. Department of Psychiatry, Dokkyo University School of Medicine, 880 Kitakobayashi, Mibu, 321-0293, Japan. Tel.: +81 282 86 1111; fax: +81 282 86 5187.
E-mail address: ozeki@dokkyomed.ac.jp (Y. Ozeki).

0278-5846/$ – see front matter © 2010 Elsevier Inc. All rights reserved.
doi:10.1016/j.pnpbp.2010.01.008

risk of QTc prolongation for an individual antipsychotic in a dose-dependent manner, particularly for second-generation antipsychotics (SGAs). Some case reports have indicated that SGAs can induce QTc prolongation (Dineen et al., 2003; Vieweg, 2003). However, such anecdotal reports do not provide clear evidence of whether SGAs increase the risk of QTc prolongation, as in first-generation antipsychotics (FGAs), in a real-world setting. This study examined the risk of QTc prolongation of antipsychotic drugs in a large clinical sample from Japan. Japan is known to use higher doses of antipsychotics (Bitter et al., 2003), providing a unique opportunity to investigate the risk of QTc prolongation in a wide range of antipsychotic doses.

2. Methods

2.1. Patients

Clinical information, including data on QTc intervals, was collected from inpatients with schizophrenia who were diagnosed according to the Diagnostic and Statistical Manual of Mental Disorders, 4th ed. (DSM-IV) in four independent hospitals. Approval from the ethics committee of each hospital was obtained. Data collection on all inpatients with schizophrenia was begun on the following dates in three psychiatric hospitals Biwako Hospital, Toyosato Hospital, and Minakuchi Hospital: February 2, 2007; February 3, 2007; and July 29, 2007, respectively. In the fourth hospital, the National Center of Neurology and Psychiatry Hospital, clinical records were collected for all patients who were admitted to its psychiatric wards between 1998 and 2007. A total of 1065 inpatients were included from the four hospitals, and all of them underwent ECG screening. Among them, 37 patients were excluded due to hypokalemia (serum potassium <3.5 mEq/L), which can induce QTc interval prolongation (Elming et al., 2003; Taylor, 2003). Two were excluded because of hypothyroidism, and nine because of cardiac disease (four patients with right bundle branch block, two with post-acute myocardial infarction, one with WPW syndrome, one with atrial–ventricular block, and one who underwent surgery for atrial septal defect). The remaining 1017 patients had a mean age of 42.6 years (S.D., 18.2) and were included in the analysis.

2.2. Procedure

A standard 12-lead ECG was recorded at 25 mm/s. Because the QTc interval is influenced by heart rate, it was corrected by Bazett's formula (QTc: $QTc = QT/RR^{1/2}$) (Bazett, 1920). An ECG recording showing the longest QTc interval was selected for each patient whose ECG was recorded two or more times. The QTc was measured automatically by a program on the ECG apparatus (MAC 5500 with 12SL algorithm by GE health care [Amersham Place, Little Chalfont, Buckinghamshire, UK]). For patients with a QTc > 430 ms, QTc and RR intervals were measured manually for the chest lead with the maximal T-wave amplitude, according to Charbit et al. (2006). The end of the T-wave was determined as the intersection between the tangent to the steepest downslope of the T-wave and the isoelectric line. QTc prolongation was defined as a QTc length of more than 470 ms in males and more than 480 ms in females, as 99% of "healthy" people can be excluded by this cut-off value (Taggart et al., 2007). One of the coauthors (M.H.), a cardiologist who specializes in arrhythmias, trained the authors on how to evaluate an ECG recording. Information on drugs administered within 24 h of the ECG recording was obtained. Table 1 shows the distribution of drugs that were administered in more than 3% of the patients and the prevalence of QTc prolongation for each medication. One hundred forty-two patients were drug free when the ECG was recorded, because they were given the test at admission before they had taken any drugs. Two hundred sixty-five patients were on monotherapy. Doses of antipsychotics, antiparkinsonian drugs, and benzodiazepines were converted into those of CP, biperiden, and diazepam equivalents, respectively (Inagaki and Inada, 2006). Subjects who were coadministered medical drugs (i.e., non psychotropic drugs) with an increased risk of producing torsade de pointes were excluded (Chan et al., 2007).

Table 1
Medication and rate of QTc prolongation in 1017 patients. Drugs which were administrated to more than 3% of patients are shown.

Administrated drugs	No. of Patients $n = 1017$ (100%)	Mean dose (SD), mg	No. of patients (%) with QTc prolongation (male: >470 ms, female >480 ms)
Equivalent dose			
CP eq.	875 (86)	963.0 (879.0)	23 (2.6)
Diazepam eq.	672 (66)	14.6 (14.6)	18 (2.7)
Biperiden eq.	645 (63)	3.8 (2.2)	19 (2.9)
Mood stabilizer			
CBZ	74 (7)	478.9 (201.8)	3 (4.1)
VPA	54 (5)	650.0 (334.1)	1 (1.9)
Lithium	47 (5)	587.2 (199.6)	4 (8.5)
Antipsychotics			
HPD	375 (37)	15.9 (12.6)	16 (4.3)
CP	299 (29)	190.5 (198.7)	9 (3.0)
LP	258 (25)	91.9 (94.5)	14 (5.4)
Risperidone	248 (24)	5.6 (3.7)	4 (1.6)
Zotepine	116 (11)	179.9 (124.9)	3 (2.6)
Olanzapine	104 (10)	15.6 (6.4)	0 (0.0)
Quetiapine	60 (6)	375.5 (258.5)	0 (0.0)
Bromperidol	49 (5)	10.7 (8.6)	0 (0.0)
Sultopride	49 (5)	1032.9 (810.2)	10 (20.4)
HPD iv	47 (5)	16.0 (10.5)	8 (17.0)

Abbreviations: eq = equivalent; HPD = haloperidol, CP = chlorpromazine; LP = levomepromazine, CBZ = carbamazepine, VPA = sodium valproate; No. = Number, SD = standard deviation.

2.3. Statistical analyses

First, logistic regression analysis was applied to examine risk factors for QTc prolongation. Age, sex, antipsychotic dose (CP equivalent), benzodiazepine dose (diazepam equivalent), and antiparkinsonian drug dose (biperiden equivalent) were included in the backward stepwise regression model. In the second analysis, age, sex, and individual antipsychotic doses were entered as independent variables in the logistic regression analysis. Then, the adjusted relative risks of important explanatory variables were calculated via the backward stepwise regression analysis. Drugs that were administrated in more than 3% of the patients were analyzed.

Linear regression analysis was used to determine which antipsychotics lengthened the QTc interval in a dose-dependent manner, as the antipsychotic dose was entered as a continuous variable. Then, the adjusted coefficients were calculated using the stepwise selection model. Age, sex, and individual antipsychotic doses were entered as independent variables.

The χ^2 test was used to examine the risk-increasing effect of excessive use of antipsychotics (cut-off points of 1000 or 1500 mg/day of CP equivalent). All statistical analyses were performed using the SPSS, version 13.0 (SPSS Japan, Inc., Tokyo, Japan). All p-values reported are two tailed. Statistical significance was considered when p-value was less than 0.05.

3. Results

The prevalence of QTc prolongation (>470 ms in male and >480 ms in female) was 2.5% (male: 3.7%; female: 1.0%). Logistic regression analysis showed that the antipsychotic dose was a significant risk factor for QTc prolongation (Table 2), whereas antiparkinsonian drugs, benzodiazepines, and mood stabilizers were not risk factors for QTc prolongation. Administration of antipsychotic doses greater than 1000 and 1500 mg/day of CP equivalent was found

Table 2
Result of logistic regression analysis on the risk of QTc prolongation for standardized doses.

	Unadjusted relative risk (95% CI)	Adjusted relative risk (95% CI)
Age	0.97 (0.94–0.99)	
Sex (risk of female)	0.33 (0.12–0.95)	
CP eq. (100 mg)	1.08 (1.05–1.12)*	1.07 (1.04–1.10)*
Diazepam eq. (1 mg)	1.01 (0.98–1.04)	
Biperiden eq. (1 mg)	0.87 (0.72–1.06)	
CBZ (100 mg)	1.00 (1.00–1.00)	
VPA (100 mg)	1.00 (0.99–1.00)	
Lithium (100 mg)	1.00 (1.00–1.01)	
	The Hosmer–Lemeshow Goodness-of-Fit Test $x^2 = 4.77$ $df = 8$ $p = 0.85$	The Hosmer–Lemeshow Goodness-of-Fit Test $x^2 = 5.15$ $df = 8$ $p = 0.74$

*$p < 0.001$.
Abbreviations: eq = equivalent, CP = chlorpromazine, CBZ = carbamazepine; VPA = sodium valproate, CI = confidence interval.

to increase the risk of QTc prolongation 1.97 fold (95% CI, 1.48–2.59, $p < 0.001$) and 2.76 fold (95% CI, 1.80–4.18, $p < 0.001$), respectively, when compared to their counterparts. On examination of individual antipsychotics, haloperidol intravenous injection (HPDiv), CP, and sultopride were found to increase the risk of QTc prolongation (Table 3).

In the stepwise selection model of the multiple linear regression analysis, CP, HPDiv, levomepromazine (LP), and sultopride were found to lengthen the QTc interval. Age was also indicated as a risk factor for QTc lengthening. Adjusted coefficients for CP, HPDiv, LP, sultopride, and sex are shown in Table 4. Adding 100 mg of LP, for example, extended the QTc interval by 4.65 ms. Bromperidol, olanzapine, quetiapine, risperidone, and zotepine had no significant lengthening effect on the QTc interval.

Table 3
Result of logistic regression analysis on the risk of QTc prolongation for each antipsychotic drug.

	Unadjusted relative risk (95%CI)	Adjusted relative risk (95%CI)
Age	0.99 (0.96–1.03)	
Sex (risk of female)	0.38 (1.26–1.16)	
HPD (2 mg)	0.99 (0.92–1.06)	
CP (100 mg)	1.37 (1.13–1.67)*	1.37 (1.14–1.64)*
LP (100 mg)	1.55 (0.92–2.61)	
Risperidone (1 mg)	1.01 (0.84–1.12)	
Zotepine (66 mg)	0.91 (0.62–1.34)	
Olanzapine (2.5 mg)	0.00 (0.00 to >100)	
Quetiapine (66 mg)	0.00 (0.00 to >100)	
Bromperidol (2 mg)	0.00 (0.00 to >100)	
Sultopride (200 mg)	1.40 (1.23–1.60)**	1.45 (1.28–1.63)**
HPD iv (2 mg)	1.26 (1.13–1.40)**	1.29 (1.18–1.43)**
	The Hosmer–Lemeshow Goodness-of-Fit Test $x^2 = 5.04$ $df = 8$ $p = 0.75$	The Hosmer–Lemeshow Goodness-of-Fit Test $x^2 = 17.81$ $df = 8$ $p = 0.013$

*$p < 0.005$.
**$p < 0.001$.
Abbreviations: HPD = haloperidol, CP = chlorpromazine, LP = levomepromazine, iv = intravenous injection, CI = confidence interval.

4. Discussion

In a large clinical sample, we confirmed that a daily dose of antipsychotics (CP equivalents) was associated with a dose-dependent increased risk of QTc prolongation; however, the use of antiparkinsonian drugs, benzodiazepines, and mood stabilizers did not significantly increase this risk. With regard to individual antipsychotics, CP, HPDiv, and sultopride were shown to significantly increase the risk of QTc prolongation. CP, HPDiv, LP, and sultopride were found to significantly lengthen the QTc interval, whereas HPD, bromperidol, olanzapine, quetiapine, risperidone, and zotepine were not.

Our observation that a daily dose of antipsychotics was associated with a risk of QTc prolongation is consistent with previous studies (Reilly et al., 2000; Warner et al., 1996). In our sample, antipsychotic doses of more than 1000 and 1500 mg/day of CP equivalents were found to increase the risk of QTc prolongation by approximately 2.0 and 3.0 fold, respectively, when compared to their counterparts. Reilly et al. also reported that a high dose (1000 to 2000 mg/day) and a very high dose (>2000 mg/day) predicted QTc prolongation [odds ratio (OR), 5.3 and 8.2, respectively] (Reilly et al., 2000). Warner et al. reported an OR of 4.3 for doses higher than 2000 mg/day (Warner et al., 1996). In contrast to antipsychotics, mood stabilizers showed no significant risk-increasing effect. This is consistent with a previous finding, which showed that lithium or carbamazepine did not significantly increase the risk of QTc prolongation (Reilly et al., 2000). However, a recent study suggested that lithium increases the QTc interval significantly (18.6 ms; 95% CI, 4.8–32.4 ms) (van Noord et al., 2009). Furthermore, lithium is known to cause T-wave changes (Mitchell and Mackenzie, 1982; Reilly et al., 2000) that may lead to torsade de pointes when combined with a QTc-lengthening antipsychotic (Liberatore and Robinson, 1984). Thus, the use of lithium requires careful ECG monitoring. With respect to valproate, our study may be the first to investigate the risk of QTc prolongation for this drug in a clinical setting. With regard to coadministered benzodiazepine and antiparkinsonian drugs, our results suggest no significant effect on QTc prolongation. Although some patients taking diazepam and biperiden equivalent showed QTc interval prolongation (Table 1), the results of logistic regression analysis showed no significant risk-increasing effect of these drugs (Table 2). Therefore, these patients were also taking chlorpromazine equivalent and it was the chlorpromazine equivalent that explained the QTc interval prolongation. Indeed, to our knowledge, there has been no study reporting that these drugs cause QTc prolongation or torsade de pointes.

With respect to individual antipsychotics, previous studies have reported that thioridazine, intravenous droperidol, sertindole, and ziprasidone are associated with a strong risk-increasing effect on QTc prolongation (Czekalla et al., 2001a; Harrigan et al., 2004; Taylor,

Table 4
QTc prolongation effect of each antipsychotic by linear regression model.

	Forced entry model	Stepwise selection model
	Coefficient (95% CI)	Coefficient (95% CI)
Age	0.19 (0.10–0.28)*	0.20 (0.11–0.29)*
Sex (risk of female)	3.22 (−0.01–6.44)	
HPD (2 mg)	0.42 (0.09–0.76)	
CP (100 mg)	3.91 (2.69–5.13)*	3.82 (2.62–5.02)*
LP (100 mg)	4.87 (2.14–7.60)*	4.65 (1.94–7.37)*
Risperidone (1 mg)	0.07 (−0.47–0.61)	
Zotepine (66 mg)	−0.36 (−1.91–1.20)	
Olanzapine (2.5 mg)	0.30 (−0.47–1.08)	
Quetiapine (66 mg)	0.11 (−0.87–1.09)	
Bromperidol (2 mg)	0.08 (−1.00–1.16)	
Sultopride (200 mg)	3.65 (2.48–4.82)*	3.56 (2.41–4.72)*
HPD iv (2 mg)	3.16 (2.36–3.96)*	3.13 (2.34–3.93)*

*$p < 0.001$.
Abbreviations: HPD = haloperidol, CP = chlorpromazine, LP = levomepromazine; iv = intravenous injection, CI = confidence interval.

2003). In Japan, commercial use of thioridazine ended in 2005; intravenous droperidol has not been used in psychiatric treatment; and sertindole and ziprasidone have not been introduced. Thus, we could not confirm the effect of these drugs. However, our results provide robust evidence that HPDiv increases the risk of QTc prolongation. This concurs with Hatta et al. who compared the differences in QTc length among psychiatric emergency patients who received intravenous flunitrazepam alone and those who received intravenous flunitrazepam and haloperidol and found that the latter group showed significantly longer QTc intervals than the former (Hatta et al., 2001). Vieweg et al. (2009) reviewed the literature and identified cases of patients aged ≥60 years who developed QTc interval prolongation, polymorphic ventricular tachycardia/torsade de pointes and/or sudden cardiac death while taking antipsychotic or antidepressant drugs or a combination of these medications. Among such cases, most frequently reported medication was HPDiv (14 out of 37 cases). These findings and ours support the recent alert of the U.S. Food and Drug Administration warning that HPDiv increases the risk of QTc prolongation and torsade de pointes based on at least 28 cases reported in the literature (U.S. Food and Drug Administration Cfdear, 2007). Oral HPD, in contrast, was found to have no statistically significant risk-increasing effect on QTc prolongation, although it had a significant QTc-lengthening effect. Previous findings have suggested that oral HPD at low or moderate doses had no clear effect on QTc, but that it is associated with QTc prolongation and torsade de pointes at higher clinical doses (>20 mg/day) (Czekalla et al., 2001a; Taylor, 2003). Taken together, excessively high blood levels of the drug after an intravenous injection or oral intake of high doses may be critical for the effect of HPD. Regarding bromperidol (oral use only), a chemically similar butyrophenone to HPD, we obtained no evidence for its effect on QTc prolongation or lengthening. To our knowledge, this is the first study to examine bromperidol for such effects. Further studies are warranted to confirm our results. With respect to CP, we detected significant effects on both QTc prolongation and QTc lengthening, which is consistent with previous findings, suggesting an intermediate effect of CP on QTc (i.e., a weaker effect than that of thioridazine, but stronger than oral HPD) (Czekalla et al., 2001a; Mehtonen et al., 1991; Witchel et al., 2003), although there have been some reports of no significant risk-increasing effect of CP (Reilly et al., 2000; Strachan et al., 2004). LP, another phenothiazine, was also found to lengthen the QTc interval in the multiple regression analysis. In the logistic regression, statistical significance was nearly achieved ($p=0.06$, Table 3). These results suggest that LP is likely to increase the risk of QTc prolongation. Although there have been little data on LP in relation to QTc in the literature, an association between sudden death and the use of phenothiazines is prominent, and LP might have been involved in such deaths (Mehtonen et al., 1991). Finally, sultopride, a benzamide derivative, was found to significantly increase the risk of QTc prolongation and QTc lengthening. To our knowledge, this is the first time that such evidence has been obtained for sultopride. Further studies are warranted to confirm our results.

Our results provide no evidence for the possible risk-increasing effect of the examined SGAs (olanzapine, quetiapine, risperidone, and zotepine) on QTc prolongation. Recently, Ray et al. (2009) reported that atypical antipsychotics double the risk of sudden cardiac death when compared with nonusers of antipsychotic drugs, a finding that contradicts our data. However, SGAs can induce weight gain, insulin resistance, and dyslipidemia (Tschoner et al., 2009), all of which are risk factors for ischemic heart diseases. Therefore, the increased sudden death observed by Ray et al. (2009) could be attributable to the increased risk of ischemic heart diseases rather than torsade de pointes due to QTc prolongation. The Pfizer 054 study (2000) reported that SGAs, such as risperidone, quetiapine, ziprasidone, and olanzapine, induced QTc interval prolongation. In the review of Czekalla et al. (2001a), it was suggested that risperidone and quetiapine could lengthen the QTc interval, although the effect observed was smaller than that of thioridazine and chlorpromazine. Olanzapine, in particular, was reported to have little effect on the QTc-interval length (Czekalla et al., 2001b). Dineen et al. (2003) reported the case of a patient who was treated with olanzapine and showed an abnormal QTc interval. Vieweg (2003) reviewed the literature and found nine cases in which QTc prolongation was associated with SGA administration (four cases of risperidone [one case was his original case], three cases of quetiapine, and two cases of ziprasidone). Taken together, although our results suggest that the SGAs (olanzapine, quetiapine, risperidone, and zotepine) are less likely to produce QTc interval prolongation than the FGAs examined herein, the SGAs can also cause QTc prolongation. Thus, further investigations with a more refined methodology are warranted. In particular, the current group-derived formula for correcting QT interval measurements to a heart rate of 60 beats per/min (QTc) are unsatisfactory (Malik, 2001), and, as pointed out by Vieweg (2003), determining the effect of drug-induced change amid the noise of random variation (regression to the mean) will require a new technology.

Female gender is known to be a risk factor for QTc prolongation (Taylor, 2003; Vieweg et al., 2009). However, we failed to detect female gender as a significant risk factor in our sample. Moreover, QTc prolongation was found more commonly in male patients than in female patients. One reason for these results was that the antipsychotic dose was substantially lower in female patients than in male patients (mean CP equivalent dose: 841 vs. 1066 mg/day; frequency of >1500 mg/day: 13.9% vs. 20.8%). In addition, because some previous studies in psychotic patients did not detect the gender difference (Chong et al., 2003; Hatta et al., 2000), such populations may have other factors that attenuate the gender difference.

There are several limitations to the study. First, we did not include medications other than psychotropic drugs in the analysis; however, the subjects included in the analysis were not coadministered other medical drugs that increased the risk for torsade de pointes (Chan et al., 2007). We also excluded patients suffering from cardiac diseases. Furthermore, psychotropic drugs that were administrated to 3% or fewer of the patients in the sample were not included in the analysis. The fact that nearly all patients received multiple drugs and a substantial proportion of participants (69%) were treated with antipsychotic polypharmacy may have made it difficult to obtain a clear result for each drug. However, there is great value in assessing the increased risk of QTc prolongation in such a practical setting. Our participants were all inpatients, and therefore individuals with severe symptomatology and those patients on high doses of antipsychotics were likely to be overrepresented. A recent study reported the possibility that an acute psychotic state itself may be a risk factor for QTc prolongation (Bar et al., 2007). Severe symptomatology might have biased the results toward an increased prevalence of the QTc interval in our subjects.

To screen QTc interval, we used an automated program, which may be fraught with errors. However, Charbit et al. (2006), for example, reported that patients with automatic QTc of <430 ms were at very low risk of having a prolonged QT interval where their definition of prolonged QTc interval was >450 ms in women and >440 ms in men. We measured QTc interval manually for patients with an automated QTc of >430 ms, although our definition of QTc prolongation was >480 ms in women and >470 ms in men. Thus, it was unlikely that we missed patients with QTc prolongation in our study. Furthermore, the reliability of the measurement algorithm of the ECG equipment (MAC 5500 with 12SL algorithm by GE health care [Amersham Place, Little Chalfont, Buckinghamshire, UK]) that we used was reported to be high. The data obtained by this algorithm was within 10 ms of the manual measurement in 95.9% of ECGs and within 15 ms in 99.3% of ECGs (Hnatkova et al., 2006). Thus, the possible effect of the use of the automated program is likely minimal. Another limitation might be that we used the chest lead with the maximal T-wave amplitude because clear T-wave leads are needed for precise

manual measurement. However, Bazett generally used limb lead II to determine his formula.

Despite these limitations, we obtained robust evidence among a large clinical sample in a real-world setting that suggested that a daily dose of antipsychotics is associated with a dose-dependent increased risk of QTc prolongation, whereas that of antiparkinsonian drugs, benzodiazepines, and mood stabilizers is not. With regard to individual antipsychotics, our results suggest that FGAs, such as HPDiv, CP, LP, and sultopride, have a risk-increasing effect on QTc prolongation and that SGAs, such as olanzapine, quetiapine, risperidone, and zotepine, are less likely to produce QTc prolongation than the FGAs. Such information may aid in clinical decision making concerning the choice of antipsychotic medication, particularly in patients who have an increased risk for arrhythmias.

5. Conclusions

We confirmed the statistical effect of chlorpromazine, levomepromazine, and HPDiv on QTc prolongation in a sample of 1017 patients with schizophrenia. Furthermore, statistical evidence for sultopride was obtained for the first time. Furthermore, in the range of the antipsychotic drugs that we examined, the data suggest that SGAs are less likely to produce QTc prolongation than FGAs, which may be useful in guiding the choice of antipsychotic drugs.

Acknowledgements

This study was supported by the Health and Labor Sciences Research Grants in Japan, Tokyo, Japan and the Dokkyo Medical University, Investigator-Initiated Research Grant (no. 2007-01-2), Mibu, Japan.

References

Bar KJ, Koschke M, Boettger MK, Berger S, Kabisch A, Sauer H, et al. Acute psychosis leads to increased QT variability in patients suffering from schizophrenia. Schizophr Res 2007;95:115–23.

Bazett HC. An analysis of the time relations of electrocardiograms. Heart 1920;7: 353–70.

Bitter I, Chou JC, Ungvari GS, Tang WK, Xiang Z, Iwanami A, et al. Prescribing for inpatients with schizophrenia: an international multi-center comparative study. Pharmacopsychiatry 2003;36:143–9.

Chan A, Isbister GK, Kirkpatrick CM, Dufful SB. Drug-induced QT prolongation and torsades de pointes: evaluation of a QT nomogram. QJM 2007;100:609–15.

Charbit B, Samain E, Merckx P, Funck-Brentano C. QT interval measurement: evaluation of automatic QTc measurement and new simple method to calculate and interpret corrected QT interval. Anesthesiology 2006;104:255–60.

Chong SA, Mythily Lum A, Goh HY, Chan YH. Prolonged QTc intervals in medicated patients with schizophrenia. Hum Psychopharmacol 2003;18:647–9.

Czekalla J, Kollack-Walker S, Beasley Jr CM. Cardiac safety parameters of olanzapine: comparison with other atypical and typical antipsychotics. J Clin Psychiatry 2001a;62(Suppl 2):35–40.

Czekalla J, Beasley Jr CM, Dellva MA, Berg PH, Grundy S. Analysis of the QTc interval during olanzapine treatment of patients with schizophrenia and related psychosis. J Clin Psychiatry 2001b;62:191–8.

Dineen S, Withrow K, Voronovitch L, Munshi F, Nawbary MW, Lippmann S. QTc prolongation and high-dose olanzapine. Psychosomatics 2003;44:174–5.

Elming H, Sonne J, Lublin HK. The importance of the QT interval: a review of the literature. Acta Psychiatr Scand 2003;107:96-101.

Faber TS, Zehender M, Just H. Drug-induced torsade de pointes. Incidence, management and prevention. Drug Saf 1994;11:463–76.

Harrigan EP, Miceli JJ, Anziano R, Watsky E, Reeves KR, Cutler NR, et al. A randomized evaluation of the effects of six antipsychotic agents on QTc, in the absence and presence of metabolic inhibition. J Clin Psychopharmacol 2004;24:62–9.

Hatta K, Takahashi T, Nakamura H, Yamashiro H, Yonezawa Y. Prolonged QT interval in acute psychotic patients. Psychiatry Res 2000;94:279–85.

Hatta K, Takahashi T, Nakamura H, Yamashiro H, Asukai N, Matsuzaki I, et al. The association between intravenous haloperidol and prolonged QT interval. J Clin Psychopharmacol 2001;21:257–61.

Hennessy S, Bilker WB, Knauss JS, Margolis DJ, Kimmel SE, Reynolds RF, et al. Cardiac arrest and ventricular arrhythmia in patients taking antipsychotic drugs: cohort study using administrative data. Bmj 2002;325:1070.

Hnatkova K, Gang Y, Batchvarov VN, Malik M. Precision of QT interval measurement by advanced electrocardiographic equipment. Pacing Clin Electrophysiol 2006;29: 1277–84.

Inagaki A, Inada I. Dose equivalence of psychotropic drugs: 2006-version. Jpn J Clin Psychopharmacol 2006;9:1443–7.

Liberatore MA, Robinson DS. Torsade de pointes: a mechanism for sudden death associated with neuroleptic drug therapy? J Clin Psychopharmacol 1984;4:143–6.

Malik M. Problems of heart rate correction in assessment of drug-induced QT interval prolongation. J Cardiovasc Electrophysiol 2001;12:411–20.

Mehtonen OP, Aranko K, Malkonen L, Vapaatalo H. A survey of sudden death associated with the use of antipsychotic or antidepressant drugs: 49 cases in Finland. Acta Psychiatr Scand 1991;84:58–64.

Mitchell JE, Mackenzie TB. Cardiac effects of lithium therapy in man: a review. J Clin Psychiatry 1982;43:47–51.

Ray WA, Meredith S, Thapa PB, Meador KG, Hall K, Murray KT. Antipsychotics and the risk of sudden cardiac death. Arch Gen Psychiatry 2001;58:1161–7.

Ray, W.A., Chung, C.P., Murray, K.T., Hall, K., Stein, C.M. Atypical antipsychotic drugs and the risk of sudden cardiac death. N Engl J Med 2009;360:225–35.

Reilly JG, Ayis SA, Ferrier IN, Jones SJ, Thomas SH. QTc-interval abnormalities and psychotropic drug therapy in psychiatric patients. Lancet 2000;355:1048–52.

Strachan EM, Kelly CA, Bateman DN. Electrocardiogram and cardiovascular changes in thioridazine and chlorpromazine poisoning. Eur J Clin Pharmacol 2004;60:541–5.

Straus SM, Bleumink GS, Dieleman JP, van der Lei J, t Jong GW, Kingma JH, et al. Antipsychotics and the risk of sudden cardiac death. Arch Intern Med 2004;164: 1293–7.

Taggart NW, Haglund CM, Tester DJ, Ackerman MJ. Diagnostic miscues in congenital long-QT syndrome. Circulation 2007;115:2613–20.

Taylor DM. Antipsychotics and QT prolongation. Acta Psychiatr Scand 2003;107:85–95.

The Pfizer 054 study; U.S. Food and Drug Administration Advisory Committee. Zeldox capsules (ziprasidone): summary of efficacy and safety and overall benefit risk relationship. Bethesda, Md: US Food and Drug Administration, Jul 19;2000.

Tschoner A, Engl J, Rettenbacher M, Edlinger M, Kaser S, Tatarczyk T, et al. Effects of six second generation antipsychotics on body weight and metabolism – risk assessment and results from a prospective study. Pharmacopsychiatry 2009;42: 29–34.

US Food and Drug Administration Cfdear. Information for healthcare professionals. Haloperidol (marketed as Haldol, Haldol Decanoate and Haldol Lactate). September 17, 2007. http://www.fda.gov/cder/drug/InfoSheets/HCP/haloperidol.htm. Accessed 2008 January 30.

van Noord C, Straus SM, Sturkenboom MC, Hofman A, Aarnoudse AJ, Bagnardi V, et al. Psychotropic drugs associated with corrected QT interval prolongation. J Clin Psychopharmacol 2009;29:9-15.

Vieweg WV. New generation antipsychotic drugs and QTc interval prolongation. Prim Care Companion J Clin Psychiatry 2003;5:205–15.

Vieweg WV, Wood MA, Fernandez A, Beatty-Brooks M, Hasnain M, Pandurangi AK. Proarrhythmic risk with antipsychotic and antidepressant drugs. Implications in the elderly. Drugs Aging 2009;26:997-1012.

Warner JP, Barnes TR, Henry JA. Electrocardiographic changes in patients receiving neuroleptic medication. Acta Psychiatr Scand 1996;93:311–3.

Witchel HJ, Hancox JC, Nutt DJ. Psychotropic drugs, cardiac arrhythmia, and sudden death. J Clin Psychopharmacol 2003;23:58–77.

KCNE2 modulation of Kv4.3 current and its potential role in fatal rhythm disorders

Jie Wu, PhD,* Wataru Shimizu, MD, PhD,† Wei-Guang Ding, MD, PhD,‡ Seiko Ohno, MD, PhD,§ Futoshi Toyoda, PhD,‡ Hideki Itoh, MD, PhD,¶ Wei-Jin Zang, MD, PhD,* Yoshihiro Miyamoto, MD, PhD,‖ Shiro Kamakura, MD, PhD,† Hiroshi Matsuura, MD, PhD,‡ Koonlawee Nademanee, MD, FACC,# Josep Brugada, MD,** Pedro Brugada, MD,†† Ramon Brugada, MD, PhD, FACC,‡‡ Matteo Vatta, PhD,§§¶¶ Jeffrey A. Towbin, MD, FAAP, FACC,§§ Charles Antzelevitch, PhD, FACC, FAHA, FHRS,‖‖ Minoru Horie, MD, PhD¶

*From the *Pharmacology Department, Medical School of Xi'an Jiaotong University. Xi'an, Shaanxi, China, †Division of Cardiology, Department of Internal Medicine, National Cardiovascular Center, Suita, Japan, ‡Department of Physiology, Shiga University of Medical Science, Ohtsu, Japan, §Department of Cardiovascular Medicine, Kyoto University of Graduate School of Medicine, Kyoto, Japan, ¶Department of Cardiovascular Medicine, Shiga University of Medical Science, Shiga, Japan, ‖Laboratory of Molecular Genetics, National Cardiovascular Center, Suita, Japan, #Department of Medicine (Cardiology), University of Southern California, Los Angeles, California, **Cardiovascular Institute, Hospital Clinic, University of Barcelona, Barcelona, Spain, ††Heart Rhythm Management Centre, Free University of Brussels (UZ Brussel) VUB, Brussels, Belgium, ‡‡School of Medicine, Cardiovascular Genetics Center, University of Girona, Girona, Spain, §§Departments of Pediatrics, Baylor College of Medicine, Houston, Texas, ¶¶Department of Molecular Physiology and Biophysics, Baylor College of Medicine, Houston, Texas, and ‖‖Masonic Medical Research Laboratory, Utica, New York.*

BACKGROUND The transient outward current I_{to} is of critical importance in regulating myocardial electrical properties during the very early phase of the action potential. The auxiliary β subunit *KCNE2* recently was shown to modulate I_{to}.

OBJECTIVE The purpose of this study was to examine the contributions of *KCNE2* and its two published variants (M54T, I57T) to I_{to}.

METHODS The functional interaction between Kv4.3 (α subunit of human I_{to}) and wild-type (WT), M54T, and I57T *KCNE2*, expressed in a heterologous cell line, was studied using patch-clamp techniques.

RESULTS Compared to expression of Kv4.3 alone, co-expression of WT *KCNE2* significantly reduced peak current density, slowed the rate of inactivation, and caused a positive shift of voltage dependence of steady-state inactivation curve. These modifications rendered Kv4.3 channels more similar to native cardiac I_{to}. Both M54T and I57T variants significantly increased I_{to} current density and slowed the inactivation rate compared with WT *KCNE2*. Moreover, both variants accelerated the recovery from inactivation.

CONCLUSION The study results suggest that *KCNE2* plays a critical role in the normal function of the native I_{to} channel complex in human heart and that M54T and I57T variants lead to a gain of function of I_{to}, which may contribute to generating potential arrhythmogeneity and pathogenesis for inherited fatal rhythm disorders.

KEYWORDS Cardiac arrhythmia; M54T variation; I57T variation; *KCNE2*; Kv4.3; Sudden cardiac death

ABBREVIATIONS CHO = Chinese hamster ovary; **HERG** = human ether-a-go-go related gene; **WT** = wild type

(Heart Rhythm 2010;7:199–205) © 2010 Heart Rhythm Society. Published by Elsevier Inc. All rights reserved.

Introduction

Classic voltage-gated K^+ channels consist of four pore-forming (α) subunits that contain the voltage sensor and ion selectivity filter[1,2] and accessory regulating (β) subunits.[3] *KCNE* family genes encode several kinds of β subunits consisting of single transmembrane-domain peptides that co-assemble with α subunits to modulate ion selectivity, gating kinetics, second messenger regulation, and the pharmacology of K^+ channels. Association of the *KCNE1* product minK with the α subunit Kv7.1 encoding *KCNQ1* forms the slowly activating delayed rectifier K^+ current I_{Ks} in the heart.[4,5] In contrast, association of the *KCNE2* product MiRP1 with the human ether-a-go-go related gene (HERG) forms the cardiac rapid delayed rectifier K^+ current I_{Kr}.[6]

The first two authors contributed equally to the original concept and the authorship of this study. This study was supported by grants from the Ministry of Education, Culture, Sports, Science, Technology Leading Project for Biosimulation to Dr. Horie; Health Sciences Research grants (H18-Research on Human Genome-002) from the Ministry of Health, Labour and Welfare, Japan to Drs. Shimizu and Horie; the National Natural Science Foundation of China (Key Program, No.30930105; General Program, No. 30873058, 30770785) and the National Basic Research Program of China (973 Program, No. 2007CB512005) and CMB Distinguished Professorships Award (No. F510000/G16916404) to Dr. Zang; and National Institutes of Health Grant HL47678 and Free and Accepted Masons of New York State and Florida to Dr. Antzelevitch. **Address reprint requests and correspondence:** Dr. Minoru Horie, Department of Cardiovascular and Respiratory Medicine, Shiga University of Medical Science, Otsu, Shiga 520-2192, Japan. E-mail address: horie@belle.shiga-med.ac.jp. (Received August 20, 2009; accepted October 7, 2009.)

1547-5271/$ -see front matter © 2010 Heart Rhythm Society. Published by Elsevier Inc. All rights reserved. doi:10.1016/j.hrthm.2009.10.012

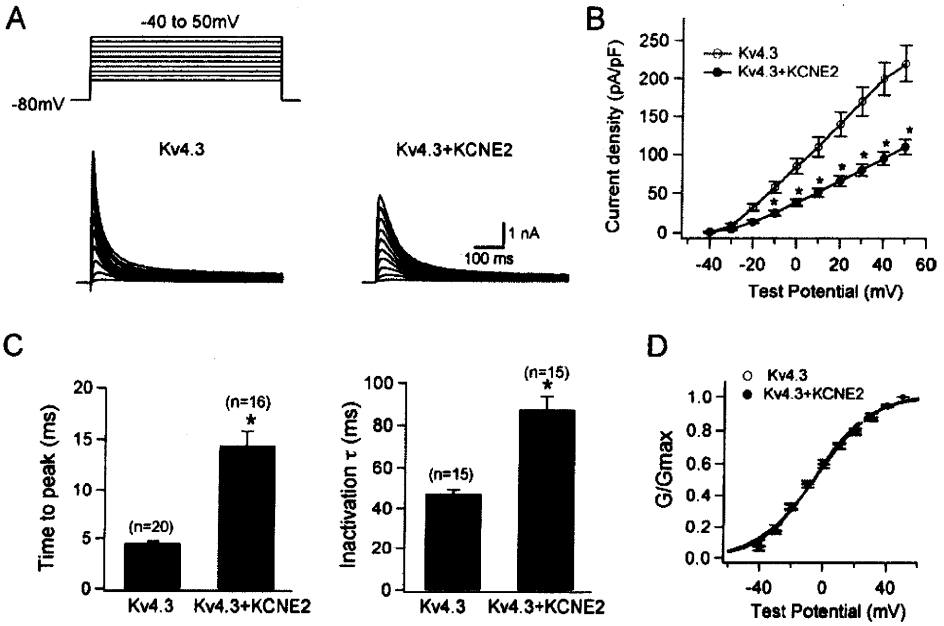

Figure 1 *KCNE2* co-expression with Kv4.3 produces smaller I_{to}-like currents with slower activation/inactivation kinetics. **A:** Representative current traces recorded from Chinese hamster ovary (CHO) cells expressing Kv4.3 **(left)** and Kv4.3 + *KCNE2* **(right).** As shown in the **inset** in panel A, depolarizing step pulses of 1-second duration were introduced from a holding potential of −80 mV to potentials ranging from −40 to +50 mV in 10-mV increments. **B:** Current–voltage relationship curve showing peak current densities in the absence and presence of co-transfected *KCNE2* (*P <.05 vs Kv4.3). **C:** Bar graphs showing the kinetic properties of reconstituted channel currents: time to peak of activation course **(left)** and inactivation time constants **(right)** measured using test potential to +20 mV (*P <.05 vs Kv4.3). Numbers in parentheses indicate numbers of experiments. **D:** Normalized conductance–voltage relationship for peak outward current of Kv4.3 and Kv4.3 + *KCNE2* channels.

Abbott et al reported that three *KCNE2* variants (Q9E, M54T, I57T) caused a loss of function in I_{Kr} and thereby were associated with the congenital or drug-induced long QT syndrome.[6,7] However, the reported QTc values in two index patients with M54T and I57T variants, both located in the transmembrane segment of MiRP1, were only mildly prolonged (390–500 ms and 470 ms).[6] We recently identified the same missense *KCNE2* variant, I57T, in which isoleucine was replaced by threonine at codon 57, in three unrelated probands showing a Brugada type 1 ECG. These findings are difficult to explain on the basis of a loss of function in I_{Kr}, thus leading us to explore other mechanisms.

Recent studies have demonstrated that interaction between α and β subunits (*KCNEs*) of voltage-gated K^+ channel is more promiscuous; for example, MiRP1 has been shown to interact with Kv7.1,[8–10] HCN1,[11] Kv2.1,[12] and Kv4.2.[13] These studies suggest that MiRP1 may also co-associate with Kv4.3 and contribute to the function of transient outward current (I_{to}) channels.[14] Indeed, a recent study reported that I_{to} is diminished in *kcne2* (–/–) mice.[15]

In the human heart, I_{to} currents are of critical importance in regulating myocardial electrical properties during the very early phase of the action potential and are thought to be central to the pathogenesis of Brugada-type ECG manifestations.[16] Antzelevitch et al demonstrated that a gain of function in I_{to} secondary to a mutation in *KCNE3* contributes to a Brugada phenotype by interacting with Kv4.3 and thereby promoting arrhythmogenicity.[14]

We hypothesized that mutations in *KCNE2* may have similar actions and characterize the functional consequences of interaction of wild-type (WT) and two mutant (I57T, M54T) MiRP1 with Kv4.3[17,18] using heterologous co-expression of these α and β subunits in Chinese hamster ovary (CHO) cells.

Methods

Heterologous expression of hKv4.3 and β subunits in CHO cells

Full-length cDNA fragment of *KCNE2* in pCR3.1 vector[10] was subcloned into pIRES-CD8 vector. This expression vector is useful in cell selection for later electrophysiologic study (see below). Two *KCNE2* mutants (M54T, I57T) were constructed using a Quick Change II XL site-directed mutagenesis kit according to the manufacturer's instructions (Stratagene, La Jolla, CA, USA) and subcloned to the same vector. Two *KCNE2* mutants were fully sequenced (ABI3100x, Applied Biosystems, Foster City, CA, USA) to ensure fidelity. Full-length cDNA encoding the short isoform of human Kv4.3 subcloned into the pIRES-GFP (Clontech, Palo Alto, CA, USA) expression vector was kindly provided by Dr. G.F. Tomaselli (Johns Hopkins University). Full-length cDNA encoding Kv channel-interacting protein (*KCNIP2*) subcloned into the PCMV-IRS expression vector was a kind gift from Dr. G.-N. Tseng (Virginia Commonwealth University). *KCND3* was transiently transfected into CHO cells together with *KCNE2* (or M54T or I57T) cDNA at equimolar ratio (*KCND3* 1.5 μg,

Table 1 Effects of *KCNE2* on Kv4.3 and Kv4.3 + KChIP2b

Parameter	Kv4.3	Kv4.3 *KCNE2*	Kv4.3 KChIP2b	Kv4.3 KChIP2b *KCNE2*
Current density at +20 mV (pA/pF)	142.0 ± 16.0 (n = 12)	66.0 ± 6.6* (n = 12)	191.5 ± 33.8 (n = 15)	77.8 ± 5.9† (n = 20)
Steady-state activation ($V_{0.5}$ in mV)	−6.5 ± 2.1 (n = 9)	−5.5 ± 1.7 (n = 11)	−7.5 ± 1.7 (n = 8)	−7.4 ± 1.4 (n = 8)
Steady-state inactivation ($V_{0.5}$ in mV)	−46.0 ± 1.3 (n = 10)	−40.8 ± 1.7* (n = 8)	−49.8 ± 1.4 (n = 7)	−44.5 ± 1.9† (n = 7)
τ of inactivation at +20 mV (τ_{inact} in ms)	47.3 ± 2.0 (n = 15)	87.2 ± 6.2* (n = 15)	47.5 ± 2.2 (n = 15)	66.6 ± 3.5† (n = 15)
Time to peak at +50 mV (TtP in ms)	4.5 ± 0.2 (n = 20)	14.4 ± 1.4* (n = 16)	4.1 ± 0.2 (n = 15)	6.1 ± 0.5† (n = 21)
τ of recovery from inactivation (ms)	419.6 ± 18.8 (n = 6)	485.6 ± 74.8 (n = 6)	89.2 ± 5.3 (n = 6)	60.2 ± 6.9† (n = 6)

*Significantly different from Kv4.3.
†Significantly different from Kv4.3 + KChIP2b.

KCNE2 1.5 μg) using Lipofectamine (Invitrogen Life Technologies, Carlsbad, CA, USA) according to the manufacturer's instructions. In one set of experiments, we also co-transfected equimolar levels of KChIP2b (*KCND3* 1.5 μg, *KCNE2* 1.5 μg, *KCNIP2* 1.5 μg). The transfected cells were then cultured in Ham's F-12 medium (Nakalai Tesque, Inc., Kyoto, Japan) supplemented with 10% fetal bovine serum (JRH Biosciences, Inc., Lenexa, KS, USA) and antibiotics (100 international units per milliliter penicillin and 100 μg/mL streptomycin) in a humidified incubator gassed with 5% CO_2 and 95% air at 37°C. The cultures were passaged every 4 to 5 days using a brief trypsin-EDTA treatment. The trypsin-EDTA treated cells were seeded onto glass coverslips in a Petri dish for later patch-clamp experiments.

Electrophysiologic recordings and data analysis

After 48 hours of transfection, a coverslip with cells was transferred to a 0.5-mL bath chamber at 25°C on an inverted microscope stage and perfused at 1 to 2 mL/min with extracellular solution containing the following (in mM): 140 NaCl, 5.4 KCl, 1.8 $CaCl_2$, 0.5 $MgCl_2$, 0.33 NaH_2PO_4, 5.5 glucose, and 5.0 HEPES; pH 7.4 with NaOH. Cells that emitted green fluorescence were chosen for patch-clamp experiments. If co-expressed with *KCNE2* (or its mutants), the cells were incubated with polystyrene microbeads precoated with anti-CD8 antibody (Dynabeads M450, Dynal, Norway) for 15 minutes. In these cases, cells that emitted green fluorescence and had attached beads were chosen for electrophysiologic recording. Whole-cell membrane currents were recorded with an EPC-8 patch-clamp amplifier (HEKA, Lambrecht, Germany), and data were low-pass filtered at 1 kHz, acquired at 5 kHz through an LIH-1600 analog-to-digital converter (HEKA), and stored on hard disk using PulseFit software (HEKA). Patch pipettes were fabricated from borosilicate glass capillaries (Narishige, Tokyo, Japan) using a horizontal microelectrode puller (P-97, Sutter Instruments, Novato, CA, USA) and the pipette tips fire-polished using a microforge. Patch pipettes had a resistance of 2.5 to 5.0 MΩ when filled with the following pipette solution (in mM): 70 potassium aspartate, 50 KCl, 10 KH_2PO_4, 1 $MgSO_4$, 3 Na_2-ATP (Sigma, Japan, Tokyo), 0.1 Li_2-GTP (Roche Diagnostics GmbH, Mannheim, Germany), 5 EGTA, and 5 HEPES (pH 7.2).

Cell membrane capacitance (C_m) was calculated from 5 mV-hyperpolarizing and depolarizing steps (20 ms) applied from a holding potential of −80 mV according to Equation 1[19]:

$$C_m = \tau_c I_0 / \Delta V_m (1 - I_\infty / I_0), \quad (1)$$

where τ_c = time constant of capacitance current relaxation, I_0 = initial peak current amplitude, ΔV_m = amplitude of voltage step, and I_∞ = steady-state current value. Whole-cell currents were elicited by a family of depolarizing voltage steps from a holding potential of −80 mV. The difference between the peak current amplitude and the current at the end of a test pulse (1-second duration) was referred to as the transient outward current. To control for cell size variability, currents were expressed as densities (pA/pF).

Steady-state activation curves were obtained by plotting the normalized conductance as a function of peak outward potentials. Steady-state inactivation curves were generated by a standard two-pulse protocol with a conditioning pulse of 500-ms duration and obtained by plotting the normalized current as a function of the test potential. Steady-state inactivation/activation kinetics were fitted to the following Boltzmann equation (Eq. 2):

$$Y(V) = 1/(1 + \exp[(V_{1/2} - V)/k]), \quad (2)$$

where Y = normalized conductance or current, $V_{1/2}$ = potential for half-maximal inactivation or activation, respectively, and k = slope factor.

Data relative to inactivation time constants, time to peak, and mean current levels were obtained by using current data recorded at +50 mV or +20 mV. Recovery from inactivation was assessed by a standard paired-pulse protocol: a 400-ms test pulse to +50 mV (P1) followed by a variable

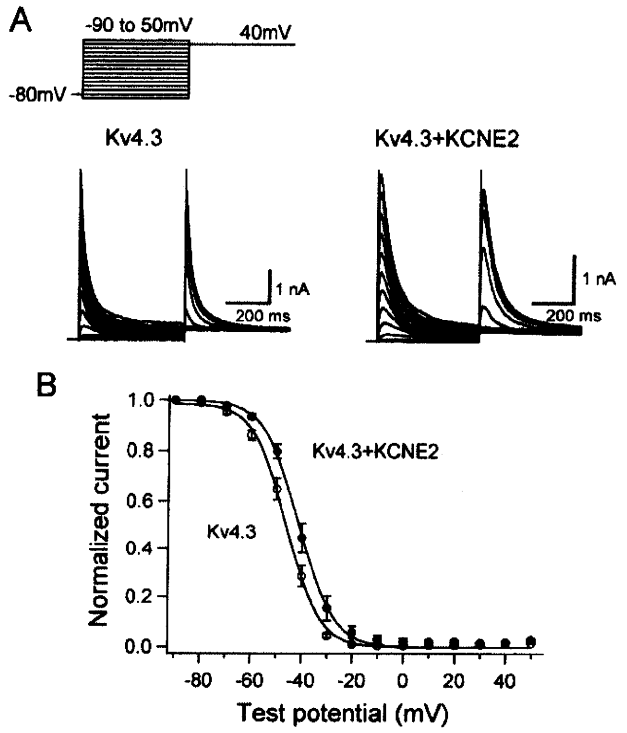

Figure 2 *KCNE2* co-expression with Kv4.3 causes a positive shift of voltage dependence of steady-state inactivation. **A:** Representative Kv4.3 and Kv4.3 + *KCNE2* current traces induced by 500-ms pulses (P1) from −90 to +50 mV applied from the holding potential −80 mV in 10-mV steps followed by a second pulse (P2) to +40 mV. **B:** Steady-state inactivation curves for Kv4.3 *(open circles)* and Kv4.3 + *KCNE2 (closed circles)* channels.

recovery interval at −80 mV and then a second test pulse to +50 mV (P2). Both the inactivation time constants and the time constant for recovery from inactivation were determined by fitting the data to a single exponential (Eq. 3):

$$I(t) \text{ (or P2/P1)} = A + B_{exp}(-t/\tau), \quad (3)$$

where I(t) = current amplitude at time t, A and B = constants, and τ = inactivation time constant or time constant for recovery from inactivation. For measurement of recovery from inactivation, the plot of P2/P1 instead of I(t) was used.

All data were given as mean ± SEM. Statistical comparisons between two groups were analyzed using Student's unpaired t-test. Comparisons among multiple groups were analyzed using analysis of variance followed by Dunnett test. $P < .05$ was considered significant.

Results

Effects of *KCNE2* on Kv4.3 currents and its gating kinetics

WT *KCNE2* initially was co-expressed with *KCND3*, the gene encoding Kv4.3, the α subunit of the I_{to} channel,[17,18] in CHO cells. Figure 1A shows representative whole-cell current traces recorded from cells transfected with *KCND3* and co-transfected with (right) or without (left) *KCNE2*. Cells expressing Kv4.3 channels alone showed rapidly activating and inactivating currents. Co-expression of *KCNE2* significantly reduced peak current densities as summarized in the current–voltage relationship curve shown in Figure 1B and slowed both activation and inactivation kinetics (Table 1). Figure 1C (left) shows mean time intervals from the onset of the pulse to maximum current (time to peak), whereas the right panel shows time constants of inactivation (at +20 mV) obtained using Equation 3. Thus, co-transfection of *KCNE2* significantly increased both the time to peak and the time constant.

In contrast, *KCNE2* did not affect the voltage dependence of steady-state activation as assessed by plotting the normalized conductance as a function of test potential (Figure 1D). Fitting to the Boltzmann equation (Eq. 2) yielded half-maximal activation potentials of −6.5 ± 2.1 mV for Kv4.3 alone (open circles) and −5.5 ± 1.7 mV for Kv4.3 + *KCNE2* channels (filled circles, P = NS; Table 1). These findings are consistent with those previously reported for studies using *Xenopus* oocytes, CHO cells, and HEK293 cells.[20,21]

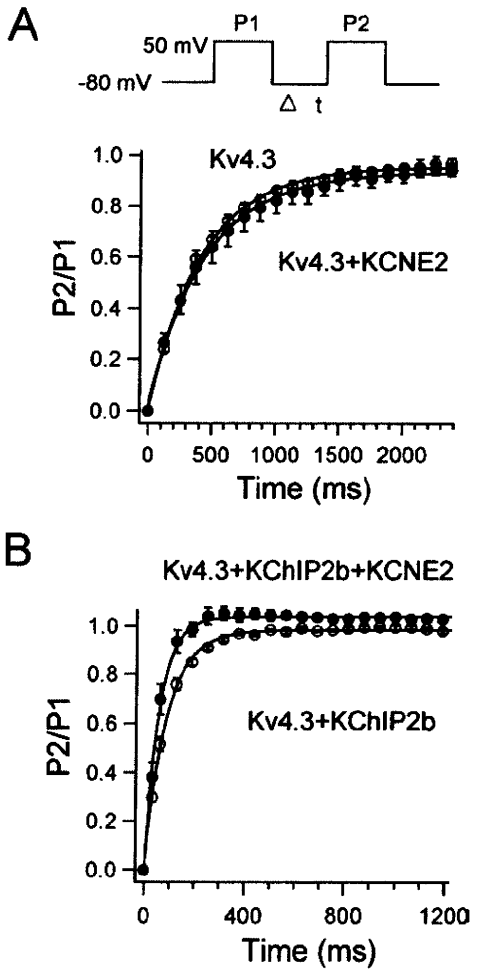

Figure 3 Effects of *KCNE2* co-expression on recovery from inactivation of Kv4.3 **(A)** and Kv4.3 + KChIP2b **(B)** currents. Recovery from inactivation was assessed by a two-pulse protocol **(A, inset):** a 400-ms test pulse to +50 mV (P1) followed by a variable interval at −80 mV, then by a second test pulse to +50 mV (P2). Data were fit to a single exponential.